

# Kinematics of W UMa-type binaries and evidences on the two types of formation

S. B ilir,<sup>1,2</sup> Y . Karatas<sup>1</sup>, O . Demircan<sup>2Y</sup> and Z . Eker<sup>2Y</sup>

<sup>1</sup>Istanbul University Science Faculty, Department of Astronomy and Space Sciences, 34119, University-Istanbul, Turkey

<sup>2</sup>Canakkale University, Ünalpasar Astronomical Observatory, 17100 Canakkale, Turkey

arXiv:astro-ph/0411291v1 11 Nov 2004

20 March 2024

## ABSTRACT

The kinematics of 129 W UMa binaries is studied and its implications on the contact binary evolution is discussed. The sample is found to be heterogeneous in the velocity space that kinematically younger and older contact binaries exist in the sample. Kinematically young (0.5 Gyr) sub-sample (MG) is formed by selecting the systems which are satisfying the kinematical criteria of moving groups. After removing the possible MG members and the systems which are known to be members of open clusters, the rest of the sample is called Field Contact Binaries (FCB). The FCB has further divided into four groups according to the orbital period ranges. Then a correlation has been found in the sense that shorter period less massive systems have larger velocity dispersions than the longer period more massive systems. Dispersions in the velocity space indicates 5.47 Gyr kinematical age for the FCB group. Comparing with the old chromospherically active binaries (CAB), presumably detached binary progenitors of the contact systems, the FCB appears to be 1.61 Gyr older. Assuming an equilibrium in the formation and destruction of CAB and W UMa systems in the Galaxy, this age difference is treated as empirically deduced lifetime of the contact stage. Since the kinematical ages (3.21, 3.51, 7.14 and 8.89 Gyr) of the four subgroups of FCB are much longer than the 1.61 Gyr lifetime of the contact stage, the pre-contact stages of FCB must dominantly be producing the large dispersions. The kinematically young (0.5 Gyr) MG group covers the same total mass, period and spectral ranges as the FCB. But, the very young age of this group does not leave enough room for pre-contact stages, thus it is most likely that those systems were formed in the beginning of the main-sequence or during the pre-main-sequence contraction phase, either by a session process (Roxburgh 1966) or most probably by fast spiraling in of two components in a common envelope.

**Key words:** binaries: eclipsing, stars: binaries spectroscopic, stars: evolution, stars: kinematics

## 1 INTRODUCTION

The low mass contact binaries, popularly known as W Ursa Majoris stars, are easily recognized by their eclipsing light curves with equal (or nearly equal) minimum as wide as to touch one another. With a small orbit implied by a short orbital period less than a day, the binary components fill their Roche lobes so that the dumbbell-shaped stars touch each other at the inner Lagrangian point. The W UMa

systems have spectral types ranging from late A to middle K and they are located near or just above the main sequence. The strong tidal interaction synchronized their rotation thus the period of rotation is equal to the orbital revolution. The rapid rotation and convective atmospheres are primary causes to their observed chromospheric and coronal emissions as well as to the presence of large starspots which are the manifestations of strong, dynamically-generated magnetic activity.

The rapid rotation and quickly changing radial velocity, on the other hand, is a serious obstacle to obtain a reliable radial velocity from the highly broadened and blended spectral lines of numerous W UMa systems. Therefore, forming

? E-mail: sbilir@istanbul.edu.tr

Y Visiting Astronomer, Istanbul University Science Faculty, Department of Astronomy and Space Sciences

a complete sample for studying galactic space motions and kinematics of W UMa stars is limited with the availability of the radial velocity measurements. From the identified 374 W UMa binaries (Kukarkin et al. 1971; van't Veer 1975) in the 3rd General Catalog of Variable Stars (GCVS), Guinan & Bradstreet (1988) were able to collect only 34 systems with a measured center of mass velocity. The number of stars classified as EW (eclipsing binaries of W UMa type) increased to 561 in the 4th edition of GCVS. But there were only 78 systems available with complete physical parameters which were studied statistically by Maceroni & van't Veer (1996). Only 37 out 78 had spectroscopic mass ratio determined from the radial velocities. Finally, Aslan et al. (1999) counted 125 W UMa binaries in the Hipparcos Catalogue, but there were only 34 binaries from which the space motions can be computed. The revised 4th edition of GCVS now contains 751 W UMa. Thanks to the dedication of David Dunlap Observatory (DDO), where 54 per cent of current radial velocities came from, and Dominion Astrophysical Observatory (DAO) with 20 per cent contribution, and the improvements of spectroscopic techniques for measuring radial velocities that a total of 129 W UMa systems were collected for this study. Nearly four times the number and the improved accuracy of data justified us to repeat previous attempts of studying kinematics of W UMa binaries.

With a small sample of less accurate data, Guinan & Bradstreet (1988) estimated a kinematical age of 8–10 Gyr for W UMa systems. If this age is compared to the 5 Gyr average age of chromospherically active binaries (CAB), classical RS CVn and BY Dra systems (Eker 1992), W UMa stars appear two times older. Nevertheless, this age of W UMa binaries was found consistent with the theory of contact binary formation from the detached binary progenitors, presumably from the short period ( $P < 5$  days) RS CVn binaries, by a mechanism involving angular momentum loss and orbital period decrease previously suggested by Huang (1967), Mestel (1968), Okamoto & Sato (1970), van't Veer (1979) and Vilhu & Raunen (1980). But, according to the space velocities and dispersions computed by Aslan et al. (1999), W UMa binaries cannot be older than RS CVn systems. This means that W UMa binaries could not have evolved from detached binaries unless the time to reach contact stage is very short.

With no pre-contact stage, there is an opposing theory which predicts the formation of contact binaries directly by a ssion process (Roxburgh 1966) at the end of the pre-main sequence contraction. Considering the brief lifetime of the contact stage ( $0.1 < t_{\text{contact}} < 1$  Gyr) estimated by Guinan & Bradstreet (1988), this theory would fail to produce older populations of W UMa binaries unless the angular momentum of contact binaries is conserved. However, with the conservation of the orbital angular momentum, this theory would refuse the formation of the contact binaries from the detached binary progenitors.

Apparently, an empirical evidence implying whether the total orbital angular momentum is conserved or not within the evolutionary time scale is extremely important to reveal the actual working model. Inspired by the predictions of Demircan (1999), Karatas et al. (2004) presented such an evidence recently from the kinematics of CAB sample containing RS CVn and BY Dra stars. The evidence of orbital

period decrease, connected to mass and angular momentum loss, was shown by comparing the total mass ( $M_1 + M_2$ ) and period histograms between the kinematically younger (age 0.95 Gyr) and the older (age 3.86 Gyr) CAB sub samples. The orbital period decrease was also indicated by the fact that the shorter orbital period systems were found older than the longer orbital period systems. According to a preliminary investigation of Demircan et al. (2004), the period decrease is exponential in time so that the active detached binaries, up to about 5 days orbital period, could change into contact form within less than about 5 Gyr. Therefore, the formation of W UMa stars from detached binaries is evidently occurring. Nevertheless, this does not mean this is the only mechanism to form contact binaries. It may still possible that a limited fraction W UMa systems, possibly the very young ones, may be forming by the ssion process.

In the present work, the kinematics of W UMa binaries is studied and its implications on the contact binary evolution is discussed. The present sample has been found heterogeneous like the CAB sample in a sense that there are younger ( $< 1$  Gyr age) and older ( $> 6$  Gyr age) W UMa binaries covering the same range of spectral types and orbital periods. The evidence of mass and angular momentum loss causing orbital period decrease during contact binary evolution has been investigated for a preliminary step as done by CAB sample by Karatas et al. (2004) by comparing the total mass ( $M_1 + M_2$ ) and period histograms between the younger and the older sub samples.

## 2 DATA

Among the 751 recorded W UMa binaries in the recently revised 4th edition of GCVS, 129 systems were found to have radial velocities. After compiling the rest of the basic data (parallaxes and proper motions), the sample is listed in Table 1, which is self-explanatory, with the columns: order number, name, HD and Hipparcos reference numbers, celestial coordinates (ICRS 2000), proper motions, parallaxes and radial velocities. The associated standard errors are given besides the related parameter. The reference numbers in the last column are separated into three fields with semicolons to indicate where the basic data were taken. The two or more reference numbers in a field indicate the sub fields, that is, there are multiple references.

### 2.1 Parallaxes and proper motions

The parallaxes and the proper motions in Table 1 were mostly taken from the Hipparcos and Tycho Catalogs (ESA 1997) and the Tycho Reference Catalog (Hog et al. 1998). The parallax and the proper motion components of three stars (TX Cnc, EE Cet, BL Eri) were taken from Roese & Bastian (1988). Among the 129 systems in Table 1, the 25 binaries do not have any trigonometric parallax, and the 12 binaries have a large relative uncertainty ( $\sigma > 0.5$ ) in the parallax measurements. Considering the fact that Hipparcos measurements are reliable up to 500 pc (two-sigma detection limit  $< 1$  mas, Perryman et al. 1997), we decided to discard the parallaxes of five (AQ Tuc, TY Pub, XZ Leo, AG Vir, RZ Com) systems since their measured parallaxes indicate a distance further than 500 pc. These

Table 1. Hipparcos astrometric and radial velocity data of the W UMa stars.

ID	Name	HD	H IP	(2000) (h m s)	(2000) ° ′ ″	cos (mas yr⁻¹)	(mas yr⁻¹)	(mas)	(km s⁻¹)	References				
1	AQ Tuc	1372	1387	00 17 21.51	71 54 56.84	28.37	1.20	-9.37	1.10	2.84	0.36	20.60	0.27	(1;5;6)
2	BH Cas			00 21 40.30	+59 12 06.60	-7.43	2.50	-32.18	2.50	3.37	0.42	-23.70	2.40	(2;5;7)
3	DZ Psc			00 36 27.93	+21 32 13.60	-6.30	2.50	14.90	2.50	4.83	0.60	-21.66	2.15	(2;5;8)
4	V 523 Cas			00 40 06.26	+50 14 15.53	146.00	2.60	-71.10	2.50	12.44	1.56	-2.54	0.90	(2;5;8;9;10)
5	AQ Psc	8152	6307	01 21 03.56	+07 36 21.63	-8.72	1.38	14.58	0.73	8.03	1.29	-12.90	0.40	(1;1;11)
6	AE Phe	9528	7183	01 32 32.93	49 31 41.29	150.93	0.80	-54.47	0.65	20.49	0.81	-9.50	2.50	(1;1;12)
7	TW Cet			01 48 54.14	20 53 34.60	44.82	3.69	-15.91	2.18	9.91	3.50	20.00	25.0	(1;1;13)
8	V 776 Cas			01 53 23.44	+70 02 33.44	19.44	1.51	4.32	1.07	4.86	1.56	-24.71	0.69	(1;1;14)
9	QX And			01 57 57.10	+37 48 23.00	12.10	2.50	-11.50	2.50	2.63	0.23	11.70	0.27	(2;5;15)
10	SS Ari			02 04 18.41	+24 00 02.23	25.60	2.50	-10.70	2.50	4.71	0.59	-3.20	1.30	(2;5;16)
11	GZ And	10270	02 12 14.07	+44 39 36.28	-15.40	2.50	-0.60	2.50	6.15	0.77	0.00	1.20	(2;5;11)	
12	V 376 And	15922	12039	02 35 11.63	+49 51 37.20	49.40	0.86	-8.28	0.66	5.07	0.89	22.83	0.89	(1;1;14)
13	EE Cet	17613	13199	02 49 52.38	+08 56 22.63	45.90	5.00	-1.00	4.90	7.29	0.91	1.60	0.93	(3;5;17)
14	UX Eri			03 09 52.74	-06 53 33.56	24.13	2.85	-3.80	1.91	6.57	2.84	12.79	1.09	(1;1;18)
15	EQ Tau			03 48 13.43	+22 18 50.94	68.40	2.50	-29.60	2.50	6.97	0.87	71.95	1.22	(2;5;14)
16	BL Eri			04 11 48.18	11 47 26.52	11.70	2.70	1.00	2.70	2.77	0.35	40.00	1.51	(3;5;19)
17	YY Eri	26609	19610	04 12 08.85	10 28 09.96	-111.87	1.46	-114.52	0.96	17.96	1.20	-15.00	1.50	(1;1;20)
18	AO Cam			04 28 13.64	+53 02 44.52	14.80	2.50	-23.30	2.50	9.20	1.15	-13.17	0.83	(2;5;18)
19	RZ Tau	285892	21467	04 36 37.66	+18 45 17.80	-26.31	1.76	-6.42	1.28	5.74	1.85	5.00	50.0	(1;1;13)
20	DN Cam	29213	21913	04 42 46.24	+72 58 41.87	-17.90	0.80	-12.98	0.50	4.49	0.89	6.04	0.98	(1;1;14)
21	V 410 Aur	280332	23337	05 01 10.84	+34 30 26.57	9.04	4.97	-5.33	2.99	4.77	5.39	36.94	3.10	(1;1;18)
22	V 402 Aur	282719	23433	05 02 14.74	+31 15 49.29	9.68	1.58	-5.84	1.05	7.01	1.31	40.82	0.93	(1;1;21)
23	AP Dor	33474	23793	05 06 45.09	59 03 03.45	56.68	1.23	77.85	0.73	4.66	0.92	6.80	0.97	(1;1;22)
24	V 1363 Ori	289949	23809	05 07 02.11	00 47 32.64	21.99	2.27	-42.58	1.50	9.47	2.36	37.89	2.02	(1;1;21)
25	ER Ori	24156		05 11 14.50	08 33 24.66	7.20	1.71	-25.73	1.14	6.24	0.78	37.90	3.30	(1;5;23)
26	RW Dor	269320	24763	05 18 32.54	68 13 32.76	96.63	2.57	55.06	1.86	8.91	1.97	66.50	1.45	(1;1;24)
27	V 781 Tau	248087	27562	05 50 13.12	+26 57 43.37	-81.59	1.51	-85.08	0.77	12.31	1.35	24.40	1.30	(1;1;25)
28	AH Aur	256902	30618	06 26 04.90	+27 59 56.40	15.21	2.23	-12.72	1.36	6.18	2.05	31.95	1.45	(1;1;26)
29	QW Gem	264672	32845	06 50 46.07	+29 27 11.34	16.57	8.12	-22.58	2.97	4.09	5.42	-0.90	1.39	(1;1;18)
30	V 753 Mon	54975	34684	07 10 57.85	03 52 43.19	-13.56	0.98	-9.14	0.66	5.23	1.04	38.58	0.83	(1;1;18)
31	TY Pup	60265	36683	07 32 46.23	20 47 31.07	-24.05	1.09	42.09	0.76	4.67	0.58	28.00	30.0	(1;5;27)
32	FG Hya		41437	08 27 03.94	+03 30 52.33	6.88	1.92	-63.68	1.40	2.92	1.90	-5.70	1.20	(1;1;11)
33	TX Cnc			08 40 01.67	+18 59 58.72	-48.20	4.00	-19.00	3.90	5.21	0.79	29.00	2.12	(3;6;8;28)
34	AH Cnc			08 51 37.87	+11 50 57.20	-7.80	2.50	-9.10	2.50	1.20	0.10	15.00	1.89	(2;6;7;29)
35	UV Lyn	44455	44455	09 03 24.12	+38 05 54.60	-71.67	1.79	18.85	1.02	8.16	1.62	-0.30	1.30	(1;1;11)
36	FN Cam	79886	46005	09 22 58.04	+77 13 10.95	-4.31	1.13	-28.56	0.74	3.62	0.95	12.96	1.11	(1;1;14)
37	EZ Hya			09 26 41.06	13 45 06.41	-30.80	3.30	-0.30	2.50	5.43	0.68	16.00	0.44	(4;5;30)
38	SAnt	82610	46810	09 32 18.39	28 37 39.97	-88.84	0.55	43.79	0.49	13.30	0.71	-5.00	1.80	(1;1;31)
39	W UMa	83950	47727	09 43 45.47	+55 57 09.08	15.55	1.03	-27.35	0.62	20.17	1.05	-29.60	1.22	(1;1;32)
40	AA UMa			09 46 59.29	+45 45 56.40	-1.00	2.50	-4.80	2.50	3.19	0.40	-34.80	1.90	(2;5;33)
41	RT Lmi			09 49 48.32	+34 27 15.40	3.60	2.50	-6.00	2.50	3.07	0.38	-10.30	1.74	(2;5;18)
42	XY Leo	49136	10 01 40.43	+17 24 32.70	56.70	1.68	-58.27	0.71	15.86	1.80	-50.00	2.00	(1;1;34)	
43	XZ Leo	49204		10 02 34.19	+17 02 47.14	-16.10	1.78	1.85	0.81	2.59	0.32	-2.03	1.43	(1;5;26)
44	Y Sex	87079	49217	10 02 47.96	+01 05 40.35	0.67	3.84	-2.67	2.05	9.02	3.38	9.80	2.00	(1;1;28)
45	ET Leo	91386	51677	10 33 25.79	+17 34 27.43	-37.71	1.53	-7.21	0.80	13.90	1.44	21.46	0.78	(1;1;17)
46	UZ Leo	52249		10 40 33.19	+13 34 00.86	-21.60	1.49	-1.10	0.89	6.27	1.59	-8.18	1.12	(1;1;26)
47	EX Leo	93077	52580	10 45 06.77	+16 20 15.68	-26.51	1.23	-37.11	0.75	9.84	1.11	-11.05	1.10	(1;1;35)
48	VY Sex	93917		10 50 29.72	02 41 43.05	-21.40	2.90	-88.60	2.20	7.34	0.92	17.47	0.79	(4;5;8)
49	AM Leo	53937		11 02 10.89	+09 53 42.69	-9.98	4.54	-29.53	3.26	13.03	3.64	5.60	1.20	(1;1;36)
50	VW Lmi	95660	54003	11 02 51.91	+30 24 54.71	12.21	0.98	-3.92	0.66	8.04	0.90	5.00	0.75	(1;1;37)
51	AP Leo	54188		11 05 05.02	+05 09 06.42	89.94	2.05	-59.58	1.17	8.26	1.70	-25.10	2.10	(1;1;11)
52	HN UMa	55030		11 15 56.38	+37 38 35.30	56.12	1.28	-35.67	0.90	5.81	1.39	-37.11	0.63	(1;1;18)
53	AW UMa	99946	56109	11 30 04.32	+29 57 52.67	-82.35	0.87	-199.74	0.68	15.13	0.90	-17.00	1.57	(1;1;38)
54	TV Mus	310730		11 39 57.76	64 48 59.29	27.00	5.20	-6.80	3.20	4.32	0.54	3.10	1.00	(4;5;39)
55	V 752 Cen	101799	57129	11 42 48.08	35 48 57.51	-53.65	1.63	-24.28	0.93	9.51	1.47	29.10	0.82	(1;1;40)
56	AG Vir	104350	58605	12 01 03.50	+13 00 30.02	-2.46	1.46	-17.64	0.56	5.02	0.63	-5.91	0.73	(1;5;41;58)
57	HX UMa	104425	58648	12 01 33.15	+43 02 29.94	65.86	2.56	-21.34	2.15	6.68	3.01	-19.88	1.11	(1;1;8)
58	CC Com			12 12 06.20	+22 31 58.00	-120.00	2.50	19.30	2.50	12.49	1.56	-10.20	1.31	(2;5;42)
59	AH Vir	106400	59683	12 14 21.00	+11 49 09.40	47.74	3.03	-107.26	1.39	10.86	3.11	6.60	0.90	(1;1;43)
60	II UMa	109247	61327	12 32 54.84	+54 47 42.89	-42.50	1.57	-12.12	1.45	5.04	1.81	-8.02	1.10	(1;1;17)
61	RW Com	61243		12 33 00.28	+26 42 58.38	-125.45	3.46	-36.05	1.89	11.45	2.45	-53.00	1.15	(1;1;44)
62	RZ Com	61414		12 35 05.06	+23 20 14.02	17.44	1.79	-11.01	1.18	4.70	0.59	-1.80	1.67	(1;5;28)
63	SX Crv	110139	61825	12 40 15.04	18 48 00.93	37.93	1.21	-5.63	0.92	10.90	1.21	8.71	0.94	(1;1;14)
64	BIC Vn		63701	13 03 16.41	+36 37 00.59	-6.38	1.23	-16.68	1.04	5.31	1.65	-5.30	1.80	(1;1;45)
65	KZ Vir	114726	64433	13 12 22.87	+02 39 13.78	-8.53	0.98	0.94	0.48	6.53	0.93	-4.50	0.48	(1;1;14)

ve stars and ER Ori, which were erroneously listed with a negative parallax, are treated like the other 25 systems without a trigonometric parallax. For them, the photometric parallaxes, which were determined from the period-color-brightness relation  $M(V) = 4.44 \log P + 3.02(B-V)_0 + 0.12$  by Rucinski (2004), were used. The photometric parallaxes were calculated with the corrections of the interstellar absorption, which were computed from the color excess as

$A_V = 3.1E(B-V)$ . Since all systems were assigned a spectral type, the color excesses were available together with their observed colors.

The Hipparcos and Tycho catalogues usually give an associated uncertainty for all of the parallax and the proper motion components measurements. However, there are 18 systems in the list without an uncertainty at the proper motion components. With an optimistic approach, we have

Table 1 { continued}

ID	Name	HD	HIP	(2000)		(2000)		cos						References				
				(h	m	s)	(	000)	(mas yr <sup>-1</sup> )	(mas yr <sup>-1</sup> )	(mas)	(km s <sup>-1</sup> )						
66	K R Com	115955	65069	13	20	15.78	+ 17	45	56.99	-6.70	0.78	-82.30	0.47	13.07	0.87	-7.86	0.38	(1;1;17)
67	H T Vir	119931	67186	13	46	06.75	+ 05	06	56.27	-107.79	3.24	-11.16	1.68	15.39	2.72	-23.38	0.68	(1;1;35)
68	X Y Boo		67431	13	49	11.57	+ 20	11	24.59	-23.32	1.87	26.91	0.89	2.94	1.70	2.11	2.02	(1;1;28)
69	V 757 Cen	120734	67682	13	51	55.74	36	37	24.82	-121.51	1.20	-61.89	0.94	14.18	1.10	50.00	2.50	(1;1;46)
70	R R Cen	124689	69779	14	16	57.22	57	51	15.65	-52.69	0.77	-22.37	0.57	9.76	0.85	-16.00	0.41	(1;1;30)
71	V W Boo		69826	14	17	26.03	+ 12	34	03.45	5.45	2.09	-48.79	0.95	3.44	1.90	23.90	0.82	(1;1;47)
72	N N Vir	125488	70020	14	19	37.74	+ 05	53	46.66	-54.17	1.09	-19.63	0.60	9.48	1.14	-6.24	0.65	(1;1;26)
73	E F Boo	234150	71107	14	32	30.54	+ 50	49	40.70	-33.23	1.17	-37.34	0.93	6.00	1.06	-13.16	1.07	(1;1;14)
74	C K Boo	128141	71319	14	35	03.76	+ 09	06	49.39	70.91	1.18	-86.58	0.80	6.38	1.34	37.04	0.75	(1;1;26)
75	G R Vir	129903	72138	14	45	20.26	06	44	04.13	-84.94	1.47	47.34	0.99	18.83	1.18	-71.72	0.89	(1;1;26)
76	A C Boo		73103	14	56	28.34	+ 46	21	44.14	-9.11	1.30	8.99	1.26	7.58	1.27	-8.60	2.20	(1;1;36)
77	T Y Boo			15	00	46.94	+ 35	07	54.89	-58.80	2.50	32.30	2.50	5.82	0.73	-41.90	1.55	(2;5;48)
78	44 Boo	133640	73695	15	03	47.30	+ 47	39	14.62	-436.26	1.36	18.93	0.98	78.39	1.03	-17.89	0.40	(1;1;35)
79	T Z Boo		74061	15	08	09.13	+ 39	58	12.86	-89.03	1.53	58.80	1.42	6.76	1.49	-36.70	1.51	(1;1;28)
80	B W Dra		74368	15	11	50.11	+ 61	51	41.26	-153.96	8.04	98.81	6.44	15.32	5.18	-60.80	1.15	(1;1;49)
81	B V Dra	135421	74370	15	11	50.36	+ 61	51	25.32	-162.57	2.98	99.13	2.47	14.86	2.56	-61.45	1.45	(1;1;49)
82	F I Boo	234224	75203	15	22	05.97	+ 51	10	55.33	-36.87	2.46	47.43	2.29	9.52	2.10	-30.55	0.72	(1;1;35)
83	O U Ser	136924	75269	15	22	43.47	+ 16	15	40.74	-387.51	0.91	2.80	0.77	17.31	0.95	-64.08	0.41	(1;1;18)
84	V Z Lib		76050	15	31	51.76	15	41	00.19	-15.61	2.55	-1.94	1.75	4.92	1.96	-31.11	2.30	(1;1;35)
85	F U Dra		76272	15	34	45.21	+ 62	16	44.28	-255.85	1.18	15.61	1.11	6.25	1.09	-11.38	1.14	(1;1;18)
86	Y Y CrB	141990	77598	15	50	32.43	+ 37	50	07.56	-74.09	0.92	10.93	0.71	11.36	0.85	-4.58	1.02	(1;1;18)
87	A U Ser			15	56	49.47	+ 22	16	01.59	-31.40	2.50	-48.60	2.50	5.46	0.68	-62.90	1.50	(2;5;36)
88	V 842 Her			16	06	02.34	+ 50	11	12.10	-27.90	2.50	20.70	2.50	6.08	0.76	-57.98	1.55	(2;5;26)
89	B X Dra		78891	16	06	17.37	+ 62	45	46.10	-7.80	1.11	7.55	0.92	3.38	1.15	-26.11	3.43	(1;1;21)
90	V 899 Her	149684	81191	16	35	01.96	+ 33	12	47.77	39.09	0.72	-39.57	0.55	8.06	0.77	-16.84	1.30	(1;1;35)
91	V 502 Oph	150484	81703	16	41	20.86	+ 00	30	27.37	-27.95	1.76	20.92	0.86	11.84	1.17	-42.56	0.85	(1;1;21)
92	V 918 Her	151701	82253	16	48	24.18	+ 17	07	59.63	-15.88	0.88	14.27	0.62	8.70	0.93	-25.72	0.74	(1;1;21)
93	V 921 Her	152172	82344	16	49	31.24	+ 47	06	28.81	7.46	0.98	5.15	0.91	2.39	0.97	-79.04	1.05	(1;1;8)
94	V 829 Her			16	55	47.88	+ 35	10	57.60	-11.80	3.10	-15.60	2.60	13.53	0.54	-13.40	1.00	(4;6;9;11)
95	V 2357 Oph		82967	16	57	16.76	+ 10	59	51.38	0.51	1.80	-103.60	1.11	5.37	2.01	-19.12	1.64	(1;1;8)
96	A K Her	155937	84293	17	13	57.82	+ 16	21	00.61	26.24	2.23	-47.63	1.99	10.47	2.77	-13.00	15.0	(1;1;50)
97	V 728 Her			17	18	04.46	+ 41	50	40.40	-14.40	2.50	-10.10	2.50	2.41	0.30	34.40	0.80	(2;5;51)
98	G M Dra	238677	84837	17	20	21.88	+ 57	58	27.00	77.21	1.13	-59.05	1.02	10.16	0.88	9.12	1.63	(1;1;17)
99	V 2377 Oph	159356	85944	17	33	56.05	+ 08	09	57.81	-12.87	1.00	-59.16	0.72	10.09	1.22	-25.79	0.38	(1;1;35)
100	V 535 Ara	159441	86306	17	38	05.55	56	49	17.29	-76.64	0.90	-49.51	0.50	8.87	0.90	-17.60	0.60	(1;1;52)
101	V 2388 Oph	163151	87655	17	54	14.17	+ 11	07	50.01	-70.81	0.87	-163.11	0.50	14.72	0.81	-25.88	0.52	(1;1;17)
102	V 566 Oph	163611	87860	17	56	52.41	+ 04	59	15.32	54.04	1.17	73.92	0.77	13.98	1.11	-42.95	1.13	(1;1;53,66)
103	V 972 Her	164078	87958	17	58	05.00	+ 32	38	53.02	-34.42	0.51	-28.43	0.46	16.25	0.61	3.98	0.46	(1;1;17)
104	V 508 Oph		88028	17	58	48.62	+ 13	29	46.27	-14.62	1.88	-45.07	1.38	7.68	2.14	-36.40	2.05	(1;1;54)
105	E F Dra			18	05	30.48	+ 69	45	15.71	-13.60	2.70	-24.40	2.40	5.74	0.72	-42.20	3.50	(4;5;11)
106	V 839 Oph	166231	88946	18	09	21.27	+ 09	09	03.63	-32.48	1.33	3.23	1.03	8.09	1.44	-63.76	0.32	(1;1;55)
107	eps Cra	175813	93174	18	58	43.38	37	06	26.48	-132.25	1.46	-110.45	0.55	33.43	0.92	57.90	1.20	(1;1;56)
108	V 401 Cyg		95816	19	29	20.27	+ 30	24	28.48	-4.96	8.70	-12.59	5.99	11.55	8.04	25.53	2.14	(1;1;17)
109	V 2082 Cyg	183752	95833	19	29	30.07	+ 36	17	14.93	20.17	0.53	94.83	0.50	11.04	0.56	-34.12	0.58	(1;1;21)
110	V 417 Aql		96349	19	35	24.12	+ 05	50	17.66	-1.90	2.86	-24.45	1.50	7.65	2.35	-14.20	1.40	(1;1;11)
111	O O Aql	187183		19	48	12.65	+ 09	18	32.38	65.70	1.60	-7.90	1.60	6.52	0.82	-45.20	0.90	(4;5;57)
112	V W Cep	197433	101750	20	37	21.54	+ 75	36	01.46	309.23	1.12	539.47	0.97	36.16	0.97	-7.90	1.00	(1;1;59)
113	L S Del		199497	20	57	10.29	+ 19	38	59.23	145.40	1.90	83.40	1.80	12.71	1.59	-25.90	1.40	(4;5;11)
114	V 2150 Cyg	202924	105162	21	18	10.88	+ 30	35	21.58	2.58	1.27	-6.25	0.91	4.73	1.59	-12.82	0.45	(1;1;35)
115	H V Aqr			21	21	24.81	03	09	36.88	-63.50	1.90	-92.30	1.80	6.99	0.87	-3.77	1.25	(4;5;18)
116	V 1073 Cyg	204038	105739	21	25	03.36	+ 33	41	14.94	-4.70	2.50	-21.00	2.50	5.44	0.95	-0.80	1.10	(2;1;60)
117	K P Peg	204215	105882	21	26	41.13	+ 13	41	17.75	-2.31	2.40	-10.65	1.20	4.37	1.67	5.52	1.03	(1;1;21)
118	D K Cyg		106574	21	35	02.67	+ 34	35	45.40	-28.37	1.24	-19.29	0.93	4.42	1.78	-5.53	1.48	(1;1;26)
119	B X Peg			21	38	49.39	+ 26	41	34.20	7.10	2.50	-11.90	2.50	6.13	0.77	25.00	3.00	(2;5;61)
120	V 445 Cep	210431	109191	22	07	10.89	+ 72	22	22.26	83.91	0.51	43.90	0.42	8.95	0.50	40.69	0.95	(1;1;21)
121	B B Peg		110493	22	22	56.89	+ 16	19	27.84	19.28	2.66	-24.66	1.85	3.02	2.26	-28.90	1.40	(1;1;11)
122	V 335 Peg	216417	112960	22	52	36.18	+ 10	13	13.19	166.57	0.86	-89.35	0.65	16.26	0.86	-15.41	0.43	(1;1;21)
123	SW Lac	216598	113052	22	53	41.66	+ 37	56	18.61	88.16	1.25	10.79	0.82	12.30	1.26	-14.46	0.90	(1;1;62)
124	A B And		114508	23	11	32.09	+ 36	53	35.11	109.02	1.55	-53.56	0.94	8.34	1.48	-27.53	0.67	(1;1;21)
125	V 351 Peg	220659	115627	23	25	25.19	+ 15	41	19.14	17.43	0.90	-16.33	0.68	7.34	0.92	-8.08	0.89	(1;1;14)
126	V Z Psc		115819	23	27	48.39	+ 04	51	23.96	435.01	2.46	180.24	1.66	16.77	2.07	-4.30	1.80	(1;1;63)
127	BD + 14 5016			23	36	55.37	+											

preferred to adopt an average uncertainty  $2.5 \text{ mas yr}^{-1}$  for them, which were determined by Hog et al. (2000) for the Hipparcos stars in general. On the other hand, Rucinski (2004) estimated that the absolute magnitudes computed by the period-brightness relation of W UMa system s are within the accuracy of  $0.25 \text{ mag}$ . Therefore, a corresponding 12.5 per cent uncertainty for the photometric parallaxes were taken.

Recent investigations, both visual and spectroscopic, indicated the presence of additional components for some W UMa binaries. Trigonometric parallaxes are frequently wrong for those systems as for the brighter systems with large uncertainties in the parallaxes. We have not preferred to introduce additional uncertainties into the published data. However, for the reader who want to estimate the bias introduced by such multiple system, the W UMa's with additional components are marked in the last column of Table 5 and are shown by empty symbols in the figures.

## 2.2 Radial velocities

All W UMa binaries have circular orbits. Thus the center of mass velocity can be obtained simply by fitting a sine curve to the measured radial velocities. However, except for the four systems (TW Cet, RZ Tau, TY Pup, AK Her), all W UMa stars in our list had well determined orbital parameters so that the center of mass velocities ( $v$ ) were available with uncertainties. The center of mass velocities and the associated standard errors were listed in Table 1 with their sources. If there was more than one source available, the data in the latest source is taken since previous radial velocities were used in the later determined orbital parameters. Nevertheless, we have found the three systems (V 523 Cas, AG Vir, V 566 Oph) with multiple orbits which were determined independently from the independent data sets. For them, the weighted mean of the systemic velocities ( $v$ ) and the weighted mean of the associated errors are adopted. Only the four systems (TW Cet, RZ Tau, TY Pup, AK Her) had measured center of mass velocities but uncertainties were not available. Their uncertainties were estimated from the scatter of component velocities on the radial velocity curve. All different types of errors have been transformed to standard errors for the sake of consistency.

## 3 GALACTIC SPACE AND VELOCITY DISTRIBUTIONS

### 3.1 Sky and space distributions

There exist no program similar to that of DDO, which contributed 54 per cent of radial velocities, in the southern hemisphere, where the number of observatories already relatively less so there is a strong bias in the sky distribution of the present W UMa system s. The celestial coordinates ( $\alpha, \delta$ ) are plotted in Fig. 1a that the bias is obvious as there are 103 system s (80 per cent) in the northern and 26 system s (20 per cent) in the southern hemisphere. Unfortunately, the bias is unavoidable because 1) The present work is established on the accumulated data in the literature and it is not wise to wait for another unknown period without a clue how southern system s will be increased. 2) Eliminating

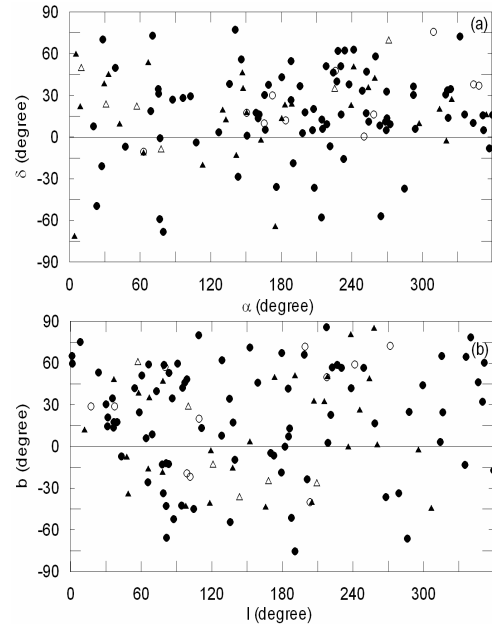


Figure 1. Sky distributions of the present sample (a) at the celestial, (b) at the galactic coordinates. Circles: Hipparcos parallaxes; Triangles: the systems use Rucinski's calibration; Filled: normal W UMa; Empty: W UMa's with visible companions.

some northern systems to establish isotropy is not feasible since it would greatly reduce the statistical significance of the sample. Due to the angle  $(63^\circ)$  between the celestial equator and the galactic plane, distribution of the sample in the galactic coordinates (Fig. 1b) appears to be less effected by the bias. Nevertheless, this is only an illusion because un-isotropy would not change by changing the coordinate system.

In order to inspect the space distributions of the present W UMa sample, the Sun centered rectangular galactic coordinates (X towards Galactic center, Y Galactic rotation, Z north Galactic Pole) were calculated. The (X, Y, Z) space coordinates are given in Table 2. The projected positions on the Galactic plane (X, Y plane) and on the plane perpendicular to it (X, Z plane) are displayed in Fig. 2. The bias on the prime reference frames (X-Y, X-Z, and Y-Z) are not that obvious as Fig. 1a. Having 69 systems with  $X < 0$  and 60 system with  $X > 0$ , the Y-Z plane shows the least bias. Having 65 and 44 systems the northern and southern Galactic latitudes, Galactic plane (X-Y) shows the strongest bias (Fig. 2) but still it is not obvious as Fig. 1a.

With a median distance of 137 pc, the sample contains relatively nearby systems and it can be considered within the Galactic thin disc. Occupying almost the same space in the Solar neighborhood, the CAB sample (Karatas et al. 2004), had a smaller median distance (98 pc) than W UMa sample. Thus, we were curious to compare space dispersions of the present W UMa sample and CAB sample. In order to avoid complications of far distant members, the space dispersions of both samples within 300 pc are calculated.

Table 2. Kinematic data of the W UMa's.

ID	Name	H D	l( )	b( )	X (pc)	Y (pc)	Z (pc)	U (km s <sup>-1</sup> )	V (km s <sup>-1</sup> )	W (km s <sup>-1</sup> )	Code	M G	O C	
1	A Q Tuc	1372	306.66	-44.97	149	-200	-249	-22.76	4.77	-45.28	4.28	-9.93	1.43	
2	B H Cas		119.08	-3.49	-144	259	-18	19.39	3.76	-15.02	2.79	-42.25	6.37	
3	D Z Psc		118.30	-41.20	-74	137	-136	3.73	2.42	-3.05	2.69	25.60	2.71	
4	V 523 Cas		121.08	-12.59	-41	67	-18	-43.78	5.37	-35.60	4.21	-28.31	3.65	
5	A Q Psc	8152	135.65	-54.53	-52	51	-101	4.38	0.70	3.94	1.57	14.81	0.81	
6	A E Phe	9528	286.22	-66.25	5	-19	-45	-20.12	0.84	-26.19	1.53	18.91	2.32	1, 1 LA , IC
7	T W Cet		190.59	-75.49	-25	-5	-98	-16.25	7.52	-20.14	7.04	-15.53	24.24	1, 1, 2 Cas, IC , LA
8	V 776 Cas		128.21	7.81	-126	160	28	-2.16	4.33	-30.62	3.90	5.20	2.95	
9	Q X And		11.91	11.43	365	77	75	-24.12	3.70	-16.87	4.41	-17.36	4.39	1, 1 LA , IC
10	S S Ari		143.57	-35.94	-138	102	-125	-16.66	2.87	-24.10	3.63	0.86	2.18	1, 1 IC , LA
11	G Z A nd		137.72	-15.87	-116	105	-44	5.46	1.90	7.72	1.89	-4.07	1.95	1 UM a
12	V 376 And	15922	139.55	-9.63	-148	126	-33	-51.49	5.50	-18.45	5.92	7.15	2.03	
13	E E Cet	17613	165.58	-43.91	-96	25	-95	-19.66	3.26	-19.71	4.03	11.64	2.87	
14	U X Eri		187.70	-51.44	-94	-13	-119	-15.59	3.79	-14.45	6.13	-2.20	3.67	1, 1 IC , LA
15	E Q Tau		168.13	-24.65	-128	27	-60	-81.50	2.42	-31.50	5.71	-14.52	2.48	
16	B L Eri		205.10	-40.70	-248	-116	-235	-32.39	3.65	-23.90	4.63	-11.85	4.04	
17	Y Y Eri	26609	203.50	-40.04	-39	-17	-36	40.04	2.22	2.37	0.57	-20.96	2.28	
18	A O Cam		152.16	2.94	-96	51	6	3.61	1.25	-18.18	1.92	-3.46	1.33	
19	R Z Tau	285892	179.21	-18.72	-165	2	-56	1.85	47.40	9.78	3.31	-20.82	17.25	
20	D N Cam	29213	137.97	17.30	-158	142	66	-12.77	1.22	9.48	1.34	-20.48	4.48	1 UM a
21	V 410 Aur	280332	170.06	-4.65	-206	36	-17	-39.23	3.88	-2.64	11.36	0.87	6.13	
22	V 402 Aur	282719	172.79	-6.45	-141	18	-16	-41.93	0.96	-1.58	1.56	-1.78	1.09	
23	A P Dor	33474	267.96	-36.37	-6	-173	-127	-82.31	17.16	-30.34	5.03	33.94	7.58	
24	V 1363 Ori	289949	201.09	-23.44	-90	-35	-42	-22.53	2.85	-34.53	5.65	-15.88	1.27	
25	E R Ori		209.20	-26.13	-126	-70	-71	-16.64	2.97	-32.93	2.67	-20.00	1.87	
26	R W Dor	269320	278.77	-33.62	14	-92	-62	-23.25	7.63	-85.23	6.89	0.64	8.40	
27	V 781 Tau	248087	182.21	-0.15	-81	-3	0	-23.71	1.30	-12.75	1.37	-43.84	4.83	
28	A H Aur	256902	185.15	7.31	-160	-14	21	-29.16	1.60	-16.32	4.75	10.01	2.54	
29	Q W Gem	264672	186.19	12.82	-237	-26	54	6.50	7.06	-30.72	41.87	6.47	12.26	
30	V 753 Mon	54975	218.61	2.56	-149	-119	9	-26.33	0.78	-25.43	0.81	-12.98	3.04	2 IC
31	T Y Pup	60265	236.04	-0.72	-120	-178	-3	-51.62	17.50	4.56	25.11	-1.09	1.11	
32	F G Hy		221.03	22.83	-238	-207	133	61.63	33.93	-78.64	53.82	-37.89	23.38	
33	T X Cnc		206.62	32.17	-145	-73	102	-42.09	3.67	-22.51	3.60	-24.46	5.27	M 44
34	A H Cnc		215.68	31.99	-574	-412	441	-6.11	7.33	-35.39	9.38	-28.54	9.59	M 67
35	U V Lyn		184.74	41.51	-91	-8	81	-27.58	5.69	12.21	2.45	-30.62	6.15	
36	F N Cam	79886	135.15	34.44	-162	161	156	-30.57	5.05	-22.65	8.09	19.53	3.45	1 LA
37	E Z Hya		245.81	25.69	-68	-151	80	-20.97	3.38	-14.28	1.31	-11.86	3.29	1, 2 LA , IC
38	S A nt	82610	258.55	16.61	-14	-71	21	-30.51	1.82	8.15	1.70	-12.40	0.80	
39	W UMa	83950	158.92	45.90	-32	12	36	21.01	0.82	-13.19	0.45	-17.29	0.91	
40	A A U Ma		173.25	49.21	-203	24	237	20.99	3.09	-9.41	3.81	-26.42	2.82	
41	R T Lmi		190.74	50.64	-203	-38	252	13.20	3.29	-6.83	3.98	-4.65	2.82	
42	X Y Leo		217.80	49.74	-32	-25	48	45.60	2.46	6.51	1.72	-32.13	1.70	
43	X Z Leo		218.44	49.80	-195	-155	295	-19.18	3.99	0.06	1.54	-18.35	3.03	1, 1 LA , Cas
44	Y Sex	87079	238.49	41.94	-43	-70	74	-0.95	1.88	-7.13	1.58	6.14	1.87	
45	E T Leo	91386	222.34	56.81	-29	-27	60	-17.73	1.15	-13.03	0.67	10.95	1.01	
46	U Z Leo		230.28	56.60	-56	-68	133	-8.66	3.55	-1.22	1.46	-14.91	2.32	1 UM a
47	E X Leo	93077	226.62	58.85	-36	-38	87	1.33	0.77	-15.00	2.24	-19.42	1.49	
48	V Y Sex	93917	253.81	48.30	-25	-87	102	15.60	2.67	-56.00	5.65	-21.28	4.39	
49	A M Leo		241.50	59.02	-19	-35	66	1.26	1.62	-12.59	3.08	-0.05	1.87	1 Cas
50	V W Lmi	95660	198.56	66.04	-48	-16	114	5.48	0.98	-0.49	0.42	7.51	0.80	1, 2 Cas, UM a
51	A P Leo		249.13	56.47	-24	-62	101	67.11	12.50	2.03	2.59	-13.45	2.39	
52	H N U Ma		179.28	67.35	-66	1	159	63.15	11.73	-11.70	2.90	-13.80	4.94	
53	A W U Ma	99946	199.11	71.93	-19	-7	63	7.01	0.54	-65.57	4.02	-22.78	1.55	
54	T V M us	310730	295.42	-2.99	99	-209	-12	34.61	6.06	10.03	2.97	0.76	3.72	
55	V 752 Cen	101799	287.63	25.01	29	-91	44	-8.12	2.97	-39.68	2.37	-5.22	2.77	
56	A G V ir	104350	260.60	0.72	-33	-197	3	11.70	1.43	-13.09	1.99	-10.20	0.94	
57	H X U Ma	104425	152.16	71.14	-43	23	142	51.86	21.15	4.70	3.77	-5.90	5.94	
58	C C Com		238.04	79.97	-7	-12	79	-41.89	5.34	-13.52	2.07	-16.34	1.51	
59	A H Vir	106400	271.52	72.39	1	-28	88	42.13	11.89	-30.79	8.29	-3.19	2.86	
60	I I U Ma	109247	128.65	62.13	-58	72	175	-29.02	10.65	-32.09	10.61	-4.69	1.45	1, 1 H ya, IC
61	R W Com		217.61	85.87	-5	-4	87	-33.71	7.99	-37.02	8.48	-56.70	1.41	
62	R Z Com		257.75	84.70	-4	-19	212	21.35	3.06	-0.24	1.39	-1.42	1.67	Com a
63	S X Crv	110139	299.25	43.99	32	-58	64	19.62	1.76	1.69	1.06	5.01	0.72	
64	B I C v n		108.86	80.19	-10	30	186	3.13	1.55	-16.11	4.86	-2.52	1.97	1 Cas
65	K Z V ir	114726	315.40	65.02	46	-45	139	-5.49	0.99	-1.82	0.67	-3.29	0.48	1, 1 UM a, Cas

Indeed, with the space dispersions of  $X = 78$ ,  $Y = 90$ , and  $Z = 87$  pc, the W UMa sample seems a little more dispersed than the CAB sample with the space dispersions of  $X = 77$ ,  $Y = 75$ , and  $Z = 73$  pc.

Considering the fact that CAB's being on average brighter than the less common W UMa's, it has been expected the opposite, since CAB's would be visible at longer distances. Obviously, the observational selection is more affected by the easy recognition of W UMa's rather than the

higher absolute brightness of CABs. Apparently, the less bright contact binaries were identified and studied more than the CAB's in similar distances.

### 3.2 Galactic space velocities

Galactic space velocity components ( $U$ ,  $V$ ,  $W$ ) were computed by applying the algorithm and the transformation matrices of Johnson & Soderblom (1987) to the basic data:

Table 2 (continued)

ID	Name	HD	$l$ ( $\circ$ )	$b$ ( $\circ$ )	X (pc)	Y (pc)	Z (pc)	U (km s $^{-1}$ )	V (km s $^{-1}$ )	W (km s $^{-1}$ )	Code	M G	O C
66	K R Com	115955	339.81	78.52	14	-5	75	13.68	1.03	-24.99	1.71	-12.35	0.49
67	H T Vir	119931	335.97	64.42	26	-11	59	-32.25	4.21	-19.12	4.16	-15.40	1.21
68	X Y Boo		8.30	75.08	87	13	329	-54.47	31.71	10.42	6.48	16.05	8.36
69	V 757 Cen	120734	316.25	24.68	46	-44	29	6.12	2.73	-66.49	3.15	12.13	1.28
70	RR Cen	124689	314.13	3.15	71	-73	6	-28.95	1.77	-8.09	1.73	-2.83	0.34
71	V W Boo		1.29	65.15	122	3	264	54.78	24.84	-46.53	25.75	1.43	11.26
72	N N Vir	125488	351.55	60.16	52	-8	91	-16.14	1.68	-24.65	3.03	0.02	0.89
73	E F Boo	234150	90.81	59.53	-1	85	144	2.98	1.23	-40.40	6.03	8.54	3.66
74	C K Boo	128141	1.46	59.62	79	2	135	89.49	14.89	-13.67	3.02	-9.34	8.71
75	G R Vir	129903	346.23	46.34	36	-9	38	-65.96	1.31	6.30	0.48	-36.32	1.19
76	A C Boo		79.26	58.76	13	67	113	-10.53	1.55	-5.11	1.32	-6.05	1.94
77	T Y Boo		57.19	61.33	45	69	151	-60.77	6.19	-32.24	2.71	-15.53	3.08
78	44 Boo	133640	80.37	57.07	1	7	11	-17.74	0.22	-26.52	0.32	-2.48	0.38
79	T Z Boo		66.21	59.00	31	70	127	-77.39	15.00	-34.97	4.05	-5.34	5.93
80	B W Dra		98.92	48.20	-7	43	49	-46.26	17.50	-60.90	7.33	-34.00	4.21
81	B V Dra	135421	98.92	48.20	-7	44	50	-49.41	9.44	-63.77	4.19	-32.77	2.56
82	F I Boo	234224	83.58	52.83	7	63	84	-33.41	6.64	-20.03	1.11	-20.57	1.25
83	O U Ser	136924	23.62	53.38	32	14	46	-90.14	3.02	-85.33	3.85	6.68	3.21
84	V Z Lib		350.03	32.15	169	-30	108	-31.88	3.54	-7.19	4.97	-9.09	3.66
85	F U Dra		97.07	45.80	-14	111	115	-104.20	17.84	-132.80	21.82	100.22	18.93
86	Y Y CrB	141990	60.49	51.14	27	48	69	-19.64	1.34	-20.46	1.48	15.69	1.66
87	A U Ser		36.85	47.84	98	74	136	-15.35	3.18	-70.45	5.81	-37.06	2.17
88	V 842 Her		78.53	46.61	22	111	120	-33.79	3.39	-47.35	2.04	-30.18	2.28
89	B X Dra		95.18	42.39	-20	218	199	-18.02	4.90	-24.07	3.20	-13.61	2.91
90	V 899 Her	149684	54.48	41.85	54	75	83	16.82	2.58	-7.59	0.89	-30.70	2.08
91	V 502 Oph	150484	17.22	28.85	71	22	41	-43.03	1.01	-11.85	0.55	-8.35	1.39
92	V 918 Her	151701	35.67	34.70	77	55	65	-26.09	0.97	-12.83	0.51	-5.68	1.11
93	V 921 Her	152172	73.07	39.89	93	307	268	-32.59	3.21	-46.14	5.14	-62.25	4.97
94	V 829 Her		57.87	37.91	31	49	45	-2.89	0.96	-13.92	1.05	-5.69	1.06
95	V 2357 Oph		30.01	30.29	139	80	94	41.96	21.92	-70.24	23.12	-43.51	12.77
96	A K Her	155937	37.51	28.73	66	51	46	6.27	11.35	-13.70	8.24	-23.09	8.52
97	V 728 Her		66.80	34.53	135	314	235	18.32	5.03	3.22	4.24	40.57	4.80
98	G M Dra	238677	86.44	34.70	5	81	56	29.12	2.72	25.10	2.05	-22.99	2.65
99	V 2377 Oph	159356	31.50	20.92	79	48	35	-5.37	2.03	-35.08	2.72	-15.51	0.88
100	V 535 Ara	159441	335.18	-13.20	100	-46	-26	-27.84	1.48	-34.51	4.23	25.82	2.26
101	V 2388 Oph	163151	36.62	17.68	52	39	21	13.72	1.95	-60.46	2.53	-9.47	0.31
102	V 566 Oph	163611	31.17	14.40	59	36	18	-51.35	1.51	5.19	2.22	-15.60	0.60
103	V 972 Her	164078	58.48	24.76	29	48	26	8.36	0.38	-5.23	0.48	8.10	0.34
104	V 508 Oph		39.37	17.66	96	79	40	-9.74	5.59	-44.05	6.25	-14.24	1.52
105	E F Dra		100.05	29.28	-27	150	85	23.06	3.21	-38.19	3.22	-10.67	2.85
106	V 839 Oph	166231	36.43	13.47	97	71	29	-51.27	0.46	-44.85	1.50	2.60	3.19
107	eps Cra	175813	359.54	-17.32	29	0	-9	58.62	1.15	-21.94	0.60	-5.98	0.51
108	V 401 Cyg		64.13	6.00	38	77	9	13.96	4.34	20.41	2.85	2.04	3.37
109	V 2082 Cyg	183752	69.40	8.70	32	84	14	-52.31	1.96	-19.09	0.84	5.75	0.60
110	V 417 Aql		43.21	-7.03	95	89	-16	-3.73	3.06	-20.52	3.50	-4.37	2.48
111	O O Aql	187183	47.82	-8.17	102	113	-22	-50.97	2.41	-25.70	1.39	-37.60	5.46
112	V W Cep	197433	109.22	20.06	-9	25	9	-74.79	2.08	-34.81	1.16	0.20	0.38
113	L S Del	199497	66.00	-16.49	31	69	-22	-67.49	6.78	-5.48	2.45	-15.62	2.89
114	V 2150 Cyg	202924	77.81	-13.04	43	201	-48	-5.65	1.37	-14.26	0.83	-3.11	2.30
115	H V Aqr		48.99	-34.47	77	89	-81	54.48	7.28	-50.34	5.94	5.91	1.35
116	V 1073 Cyg	204038	81.13	-11.95	28	178	-38	10.46	3.45	-5.33	1.43	-9.53	2.73
117	K P Peg	204215	65.75	-25.73	85	188	-99	5.53	3.88	-2.13	2.72	-7.30	2.74
118	D K Cyg		83.29	-12.76	26	219	-50	29.62	14.63	-8.34	1.87	7.08	2.64
119	B X Peg		78.21	-19.00	32	151	-53	2.52	2.00	19.22	2.91	-17.99	2.40
120	V 445 Cep	210431	111.13	13.38	-39	101	26	-63.88	2.65	20.92	1.25	1.51	0.55
121	B B Peg		78.90	-33.56	53	271	-183	-15.44	4.58	-50.75	20.31	-24.94	30.77
122	V 335 Peg	216417	81.25	-42.83	7	45	-42	-30.97	1.50	-41.28	1.63	-26.21	1.97
123	SW Lac	216598	98.68	-19.33	-12	76	-27	-31.07	3.22	-22.24	1.24	-6.60	1.25
124	A B And		101.60	-21.81	-22	109	-45	-37.31	7.05	-53.16	5.05	-38.91	8.74
125	V 351 Peg	220659	94.40	-42.37	-8	100	-92	-6.95	0.81	-16.05	1.46	-5.22	1.51
126	V Z Psc		87.50	-52.17	2	37	-47	-133.25	16.32	-12.75	1.72	-8.92	2.11
127	BD + 14 5016		97.90	-43.42	-33	235	-225	-35.15	4.56	-6.46	2.37	-8.78	2.24
128	E L A qr		81.40	-65.65	13	87	-193	4.31	3.35	8.92	2.46	-9.27	2.24
129	U Peg		104.61	-45.01	-25	95	-99	45.41	8.58	-26.60	1.85	2.41	3.73

celestial coordinates ( $l$ ,  $b$ ), proper motion components ( $U$ ,  $V$ ), radial velocity ( $W$ ) and the parallax ( $\pi$ ) of each star in Table 1, where the epoch of J2000 coordinates were adopted as described in the International Celestial Reference System (ICRS) of the Hipparcos and the Tycho Catalogues. The transformation matrices use the notation of the right handed system. Therefore, the  $U$ ,  $V$ ,  $W$  are the components of a velocity vector of a star with respect to the Sun, where the  $U$  is directed toward the Galactic center ( $l = 0^\circ$ ;  $b = 0^\circ$ ); the  $V$

is in the direction of the galactic rotation ( $l = 90^\circ$ ;  $b = 0^\circ$ ); and the  $W$  is towards the north Galactic pole ( $b = 90^\circ$ ).

Uncertainties of ( $U$ ,  $V$ ,  $W$ ) space velocity components have been computed by propagating the uncertainties of the input data (proper motions, parallax and radial velocity) by the algorithm also by Johnson & Soderblom (1987). The arithmetic mean of the uncertainties for ( $U$ ,  $V$ ,  $W$ ) are:  $U = 5.52$ ,  $V = 4.67$  and  $W = 3.75 \text{ km s}^{-1}$ . By inspecting the individual errors of space velocity vec-

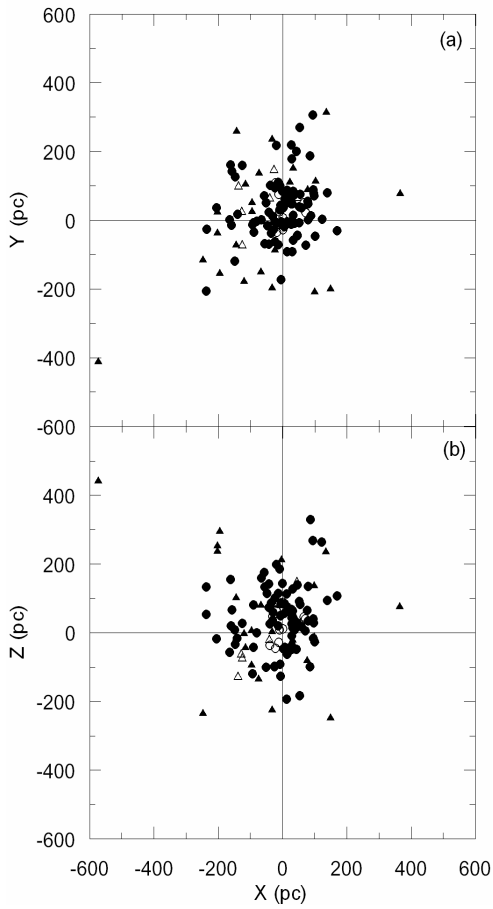


Figure 2. The space distributions with respect to the Sun.  $X$ ,  $Y$ , and  $Z$  are heliocentric galactic coordinates directed towards the Galactic Center, Galactic rotation and the North Galactic Pole. Symbols mean the same as Fig. 1.

tors ( $S = \sqrt{U^2 + V^2 + W^2}$ ), we have found only 11 (8.5 per cent) systems with the errors bigger than  $20 \text{ km s}^{-1}$ . If those systems were removed from the sample, the averages would reduce to  $U = 4.04$ ,  $V = 3.12$ , and  $W = 2.68 \text{ km s}^{-1}$ . Thus, it can be claimed confidently that most of the sample stars have the velocity uncertainties smaller than the velocity dispersions calculated. However, in comparison with the CAB sample (Karatas et al. 2004), the average uncertainties of the present WUMA sample appear nearly two times bigger. Obviously, this is the result of the lower accuracy of WUMA radial velocities because of shorter orbital periods and higher rotation rates.

Having relatively less accurate space velocities, we were curious to check the effect of the differential Galactic rotation. Thus, the first-order Galactic differential rotation contributions to the  $U$  and  $V$  components were computed as described in Mathias & Binney (1981). The  $W$  velocities are not affected in this first-order approximation. We have found 27 stars (21 per cent) with the contribution from the Galactic differential rotation being greater than the uncertainty

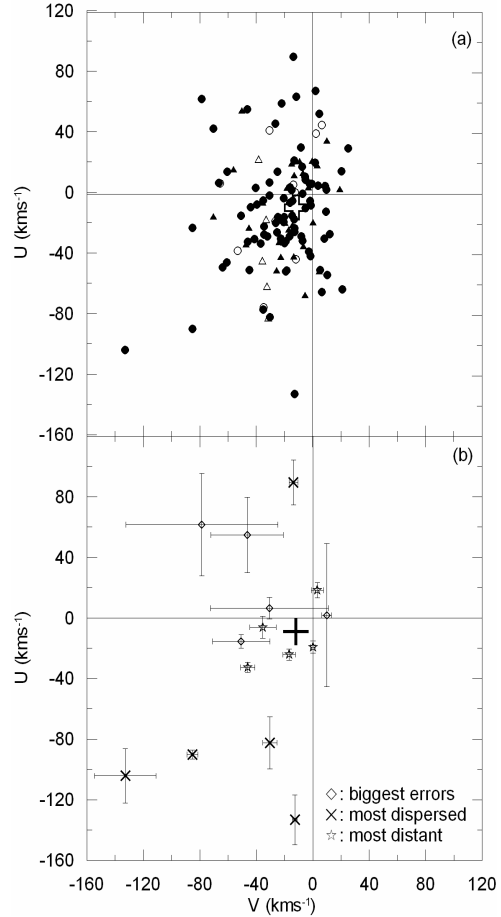


Figure 3. (a) Velocity dispersions on the  $U$ – $V$  plane. (b) propagated errors of some selected systems. Symbols in (a) are the same as Fig. 1 and symbols in (b) are self indicated. The velocities are heliocentric. The position of LSR is marked by +.

of the  $U$  component of the space velocity. The effect on the  $V$  component is rather small that the effect of Galactic differential rotation was found smaller than the uncertainties in  $V$ . Nevertheless, the Galactic differential rotation correction was applied to all of stars in the present sample. The corrected  $U$ ,  $V$ ,  $W$  are given in Table 2, together with the propagated standard errors.

There is no direct way to estimate how the un-isotropic sky distribution (bias shown in Fig. 1a) effects the WUMA space velocities. However, since present sample contains only nearby systems within the Galactic thin disc and since first-order Galactic differential rotation correction were applied, the bias seems to be minimized perhaps disappeared in the space velocity distribution. This is because the velocity distribution present WUMA sample has a great resemblance to the velocity distribution of the CAB sample (Karatas et al. 2004) which were considered homogeneously and isotropically distributed in the solar neighbourhood. Distribution of the space velocity components on the  $U$ – $V$  plane is displayed in Fig. 3a.

In order to display reliability of computed  $U$ ,  $V$ ,  $W$  velocities, Fig. 3b shows error bars some selected systems as 1) ve system which are the most distant, 2) ve systems with the biggest space velocity vector ( $S$ ), 3) ve systems which are the most dispersed on the  $U$ – $V$  diagram. It is also clear on Fig. 3b that propagated uncertainties, even the extreme cases as above, appear smaller than the dispersion thus the space velocities ( $U$ ,  $V$ ,  $W$ ) and their dispersion can be considered reliable. Nevertheless, in order to minimize the contribution of the space velocity errors, the dispersion were calculated with respect to the LSR rather than arithmetic mean of the space velocities. The position of the LSR is obtained by subtracting the Sun's velocity ( $U;V;W$ ) = (9;12;7) km s<sup>-1</sup> by Michalas & Binney (1981) from the frame of ( $U$ ,  $V$ ,  $W$ ) velocities.

### 3.3 Population analysis

As in the CAB sample (Karatas et al. 2004), we have used the parameter  $f_K = (1-300)(1.0u^2 + 2.5v^2 + 3.5w^2)^{1/2}$  to determine the possible metal-poor binaries kinematically as suggested by Green (1987) and Bartkevičius, Lazauskaite, & Bartasiūtė (1999). Here, the  $u$ ,  $v$ ,  $w$  velocities represent space velocity components with respect to the LSR. Statistically, the stars  $f_K \leq 0.35$  belong to the thin disc, the stars with  $0.35 < f_K \leq 1.00$  belong to the thick disc. The stars with  $f_K > 1$  belong to the halo population.

According to  $f_K$  analysis, the vast majority (93 per cent) of our sample are thin disc stars. The possible thick disc members are found to be 7 per cent in the current sample. The thick disc candidates are FU Dra, AP Dor, RW Dor, FG Hya, O U Ser, AU Ser, V 921 Her, V 2357 Oph, and VZ Psc. Spectroscopic metal abundances of W UMa stars appear unachievable due to fast rotation and blendings in their spectra. Photometric indices are also entirely unreliable due to the elevated magnetic activity of the W UMa systems. Nevertheless, photometric metal abundance of BW Dra has been determined by Marsakov & Shevelev (1995) ( $[m/H] = -0.56$  dex) and recently by Nordstrom et al. (2004) ( $[m/H] = -0.69$  dex) from the observations of Stromgren photometry. A 10.33 Gyr age is estimated for it by Marsakov & Shevelev (1995) according to the revised Yale isochrones ages (Green, Demarque, & King 1987). If those metal abundances and isochrone ages are correct, with the  $f_K$  kinematic value of 0.33, BW Dra appears as a star which belongs to the thick disc population although its  $f_K$  value is little less than the lower limit.

Karatas et al. (2004) had found 7 per cent of CAB binaries are possible members of the thick disc population. It is indeed interesting that the same percentage of thick disc W UMa binaries found in this study coincides with nearly the same ratio, 6 per cent of solar neighborhood stars in general belongs to the thick disc population which were found by Buser, Rong, & Karaali (1999), Siegel et al. (2002), and Karaali, Bilir, & Hamzaoglu (2004).

## 4 DISCUSSION

### 4.1 Kinematics of contact binaries

Having only the main sequence components from the spectral types A to K, the present sample of W UMa binaries appear less heterogeneous than the CAB binaries with the components F to M spectral types of all combinations of the luminosity classes from V to II. Having orbital periods from 1 days to several hundred days, the CAB sample is also considered heterogeneous (Karatas et al. 2004) regarding to the period ranges since different orbital periods may represent different evolutionary paths (Pavlov 1968, Thomas 1977). But, with a very limited range of short orbital periods ( $0.22 < P < 1.13$  days), the W UMa sample can be claimed homogeneous in a sense that all binaries with main sequence components are in the contact stage. However, the velocity distribution of W UMa sample on the  $U$ – $V$  plane (Fig. 2) appears heterogeneous as the CAB sample, that kinematically younger and older sub systems occupy the same velocity space. With the dispersions of 36.5, 26.2, 19.5 km s<sup>-1</sup> at  $U$ ,  $V$ , and  $W$  velocity components, it is possible to assign a 4.43 Gyr kinematical age to the whole sample according to the kinematical tables of Wien (1982). Karatas et al. (2004) assigned 3.86 Gyr age to the old CAB binaries. Thus, even before selecting out possible moving group (MG) members, which indeed seems to exist from the appearance of Fig. 3, the W UMa sample is little older than the CAB sample.

Guinan & Bradstreet (1988) investigated whether correlations exist between the space velocities and the physical properties of the W UMa systems, such as orbital period ( $P$ ), mass ratio ( $q$ ), system type (A or W), filling factor ( $f$ ), ultraviolet excess, and metallicity index. A weak correlation appeared possible in the sense that the space velocities tend to increase with decreasing orbital period. Also, a weak correlation appeared as binaries with large  $f$  (over-contact) tend to have higher space velocities. But, no correlation had been found between the space velocities and the mass ratio, the space velocities and the binary type (A or W), the space velocities and the metallicity index.

In order to search kinematically different sub groups, here we have preferred to divide the whole sample into two sub samples according to a criterion, then to compare their  $U$ – $V$  diagrams. The preliminary criteria and the  $U$ – $V$  diagrams are summarized and displayed in Fig. 4.

W UMa binaries with spectral types later than F7 tend to have larger dispersions (Fig. 4a and b) than W UMa's of earlier spectral types. This could be explained by the fact that the later spectral types on the H–R diagram contain older systems since evolution into the main-sequence and the duration on the main sequence is longer. However, it is indeed extraordinary that kinematically young and old systems (small and large dispersions) may well exist in both groups. Thus, this criterion fails to provide kinematically homogeneous sub samples.

W UMa stars are classified into A- or W-type systems from their light curves and radial velocity curve (Binnendijk 1970). The W-type systems are those like W UMa itself in which the hotter component (the star eclipsed at the primary minimum) is the smaller and the less massive. Comparison of the  $U$ – $V$  diagram between the A- and W-type in Fig. 4 confirms the Guinan & Bradstreet (1988) that both groups are indistinguishable kinematically, that younger and

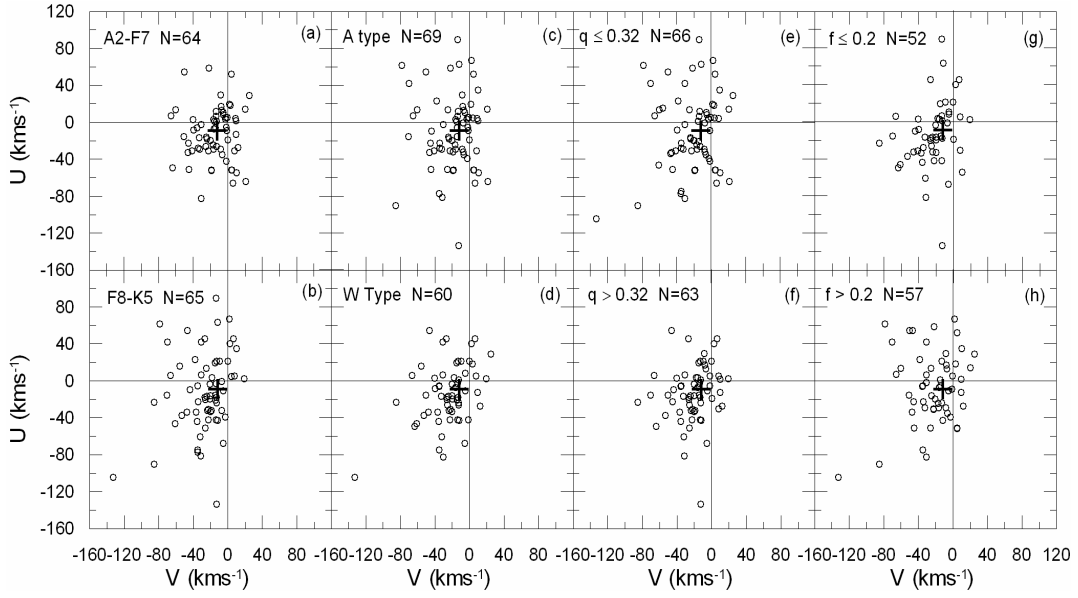


Figure 4. Comparison of the space velocity dispersions of various sub-groups on the  $U - V$  diagram. (a) earlier spectral types A 2 to F 7; (b) later spectral types F 8 to K 5; (c) A type; (d) W type; (e) mass ratio  $q \leq 0.32$ ; (f) mass ratio  $q > 0.32$ ; (g) over-contact parameter  $f \leq 0.2$ ; (h) over-contact parameter  $f > 0.2$ .

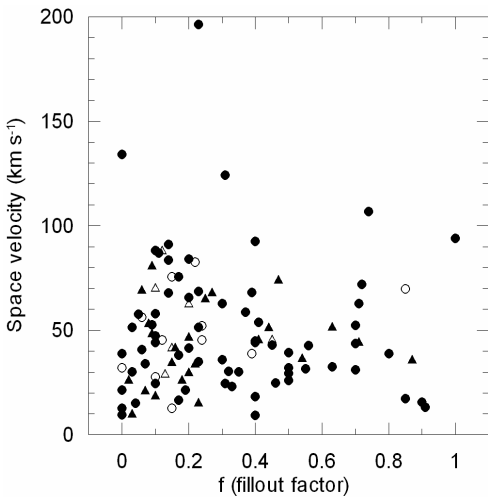


Figure 5. The space velocities is plotted against the fillout factor ( $f$ ) for WUMA binaries.

older systems are equally likely to exist in both sub-groups of A or W.

If a few high dispersion binaries are removed from the small mass ratio systems, then both sub-groups (Fig. 4e and f) of mass ratio criterion will be indistinguishable kinematically. Like the two criteria before, the mass ratio criterion also fails to distinguish younger and older systems homogeneously.

The degree of overfilling ( $f$ ) of the inner critical envelope

surface is an important parameter which may indicate a stage of an evolution for a contact binary which would coalesce into a single star. FK Com is believed by some to be the product of binary star coalescence (Bopp & Rucinski 1981, Bopp & Stencel 1981). The value of overfilling factor  $f$ , which depends on how it is defined, changes from the minimum, when the system is just in contact, to the maximum when components blow out their outer critical envelopes. Different authors define  $f$  differently, e.g. Guinan & Bradstreet (1988) define  $f$  as  $1 - f_{\text{min}}$ , but Maceroni & van't Veer (1996) define  $f$  as  $0 - f_{\text{min}}$ . Using the same definition as Maceroni & van't Veer (1996), we have found 109 systems with  $f < 0.2$ . The systems with smaller  $f$  are compared to the systems with large  $f$  on the  $U - V$  diagram (Fig. 4g and h). The systems with larger  $f$  values seem to have larger dispersions, so they appear kinematically older than the systems with smaller  $f$ . Although this is a natural consequence of the theory of coalescence into a single star, and it may appear to confirm Guinan & Bradstreet (1988), with a careful look at the  $U - V$  diagrams (Fig. 4g and h) one may notice the two sub-groups are not really homogeneous. Kinematically older and younger systems appear to exist in both groups.

In order to make a direct comparison to the Fig. 9 of Guinan & Bradstreet (1988), the space velocities ( $s = \sqrt{u^2 + v^2 + w^2}$ ) in our sample is plotted against the  $f$  values in Fig. 5. According to this presentation, the high velocity stars may well exist at low or high values of  $f$ . Thus it can be concluded that  $f$  criterion, like the criteria before (spectral type, binary type (A or W), mass ratio) is not a good criterion to differentiate kinematically older and younger WUMA binaries.

This result, however, is consistent with the very brief lifetime of a contact stage, which was predicted by Guinan

& Bradstreet (1988) as  $0.1 < t_{\text{contact}} < 1$  Gyr, and the kinematical ages of the sample as a whole which is 4.43 Gyr. The dispersions on the U-V diagram are produced in a time scale not only covering the contact stage but also covering the pre-contact stages of all. Obviously the contact stage for many W UMa stars is too short to be effective on the observed dispersions. Therefore, it is possible that a W UMa system with a longer pre-contact evolution may reach to a contact configuration at kinematically larger ages than the  $f$  value can be very small. But, on the other hand it is also possible for a W UMa system, with a much shorter pre-contact stage (small kinematical ages), to have larger value for the  $f$ . Therefore  $f$  value criterion fails to discriminate between kinematically young and old systems.

The present W UMa sample were said above to be homogeneous in a narrow range ( $0.22 < P < 1.13$  days) of the short orbital periods. However, the correlations of orbital periods with the dispersions on the U-V diagram is well presented in Fig. 6 in a sense that the short period W UMa systems have larger dispersions. The sub groups according to the total mass ( $M = M_1 + M_2$ ) display a similar correlation that less massive systems have larger dispersions than more massive systems.

All sub groups discussed above are summarized numerically in Table 3. The numerical values (velocity averages and dispersions) of the sub groups come from inspection of the dispersions on U-V diagrams on the Fig. 4 and Fig. 6. Indeed the grouping according to spectral type, system's type (A or W), mass ratio, and  $f$  value in Fig. 4 do not show very much differences in the dispersions. But grouping according to orbital period and total mass (Fig. 6) is confirmed strongly in Table 3. Using the tables of Wien (1982), a kinematical age was assigned to each hypothetical sub-group. The ages represent a mean kinematical age of all the stars in a group. The age to be meaningful depends on the meaningfulness of the group. The sub groups using orbital period and total mass criteria are indeed meaningful because the decrease of orbital period and total mass, which is established for CAB (Karatas et al. 2004), appears to be a process continuing also in the contact stage. Because of a relatively very short contact stage, there is no guarantee about the sub groups of total mass and orbital period being homogeneous. One way of selecting out younger population W UMa binaries among the sub samples according to orbital period, is to pick out possible moving group members as done in CAB sample by Karatas et al. (2004).

#### 4.2 Possible MG members among W UMa systems

Moving groups (MGs) are kinematically coherent groups of stars that share a common origin. Eggen (1994) defined a supercluster of stars gravitationally unbound in the solar neighborhood, but sharing the same kinematics while occupying the extended regions in the Galaxy. Therefore, a MG, unlike the well known open clusters covering a limited region, can be observed all over the sky. The kinematical criteria, which were originally defined by Eggen (1958a, b, 1989, 1995), for determining the possible members of the best-documented MGs are summarized by Montes et al. (2001a, b). Evidence has been found that many young and active late-type binaries can be the members of some young moving

groups (Jehres 1995, Montes et al. 2001b, King et al. 2003). Indeed, possible moving group members determined by Eggen's kinematical criteria have been proved to be very useful for separating kinematically heterogeneous CAB sample into two sub samples representing younger and older populations (Karatas et al. 2004) better than the classical approach of pre-determined sub groups with a dividing line of a chosen parameter.

The difficulty of separating kinematically young and old populations in the velocity space is obvious. The dispersions increase with age but there are always some stars naturally occupying the regions near the LSR. It is, therefore, not safe to pick stars randomly near the LSR and then to form a kinematically young group with them. Eggen's kinematical criteria, however, objectively select some stars which have space velocity vector parallel to the converging point of each pre-determined and well known MGs within an acceptable uncertainty. There are two criteria that one sets a range of the direction of the test star's proper motion and other puts limits on the test star's radial velocity vector. Fulfilling one of the criteria makes the test star a possible member. But, fulfilling both criteria does not guarantee membership since there is always a possibility that the same velocity space could be occupied by the MG members and the non-members. Further independent criteria implying a common origin and same age as the members are needed to confirm the true membership. Therefore, we should always remember that Eggen's criteria determines only the possible members of a MG. The parameters of the well-documented MGs and the possible membership criteria to them have been summarized by Karatas et al. (2004) for the CAB binaries. Here we apply the same criteria to the stars in the present W UMa sample and 28 systems were found to satisfy at least one of the criteria for one of the five MGs which were listed in Table 4. The possible moving group members among the W UMa binaries in the present sample is marked in the latest columns of Table 2 with the names of MG associated.

After determining the possible moving groups, the whole sample has been divided into three sub groups. The first one contains the possible moving group members and named MG. The second group contains only five stars which are previously known to be the members of well known open clusters. The third one is called 'Field Contact Binaries' (FCB) which contains old W UMa systems free from the possible MG and the known open cluster members in the solar neighborhood. Fig. 7 compares the U-V diagram of the MG and the FCB. The detailed kinematics and implied kinematical ages of MG and FCB are included in Table 3.

The velocity dispersions of old contact binaries (FCB) imply a mean kinematical age of 5.47 Gyr. The mean kinematical age is found to be 500 Myr for the possible MG members. Although, this age appears to be consistent with the ages of MG in Table 4, it may not represent the true mean kinematical ages of all possible MG members. This is because, the ages in Table 3 are estimated from the dispersions with respect to the LSR. In reality, each MG has its own center of dispersion which is slightly different than the LSR. Therefore, we should keep in mind that members should be at the age of each MG listed in Table 4.

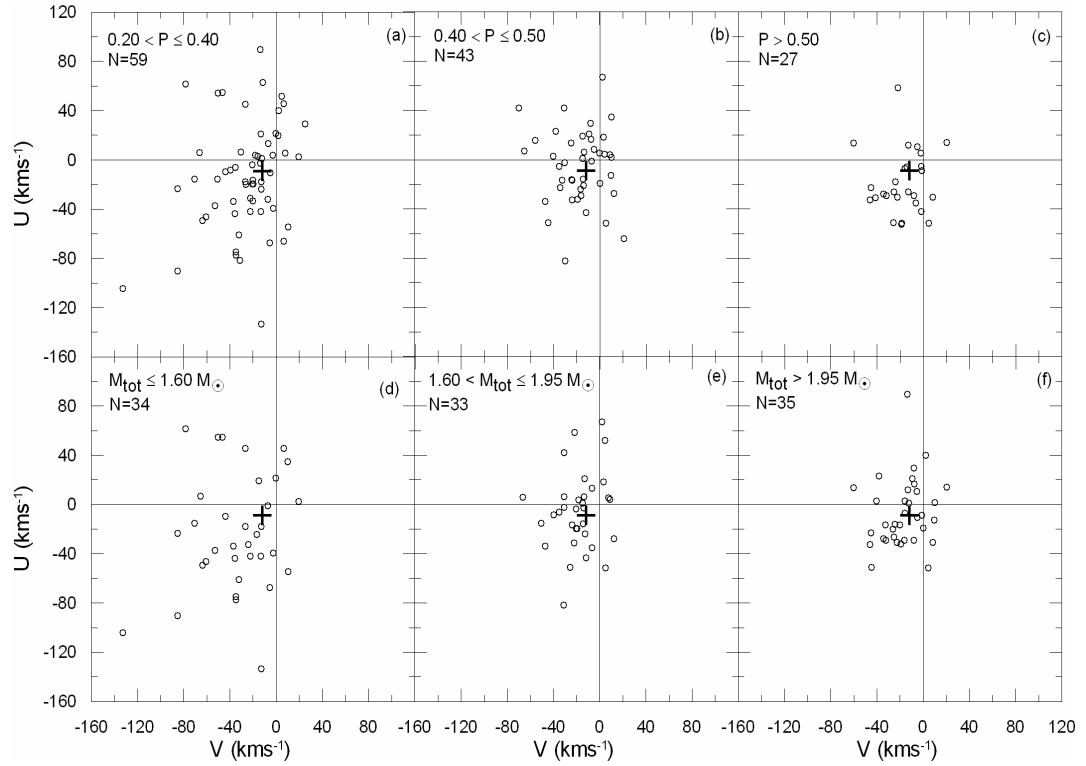


Figure 6. Comparison of the space velocity dispersions of period and total mass sub groups on the  $U$ – $V$  diagram. (a)  $0.2 < P \leq 0.4$  days; (b)  $0.4 < P \leq 0.5$  days; (c)  $P > 0.5$  days; (d)  $M_{\text{tot}} \leq 1.60 M_{\odot}$ ; (e)  $1.60 < M_{\text{tot}} \leq 1.95 M_{\odot}$ ; and (f)  $M_{\text{tot}} > 1.95 M_{\odot}$ .

Table 3. Kinematical data and the predicted kinematical ages of the sub groups of WUMa.

Data	N	$\langle U \rangle$ (km s $^{-1}$ )	$\langle V \rangle$ (km s $^{-1}$ )	$\langle W \rangle$ (km s $^{-1}$ )	$U$ (km s $^{-1}$ )	$V$ (km s $^{-1}$ )	$W$ (km s $^{-1}$ )	$v_{\text{tot}}$ (km s $^{-1}$ )	Age (G yr)							
All	129	-12.11	0.62	-21.19	0.62	-8.52	0.41	36.50	7.06	26.23	7.09	19.46	4.65	49.0	11.0	4.43
A2-F7 Spectral type	64	-12.28	0.96	-15.22	0.51	-6.16	0.55	28.94	7.68	21.34	4.11	17.22	4.43	39.9	9.8	2.83
F8-K5 Spectral type	65	-11.93	0.80	-27.07	1.12	-10.85	0.60	42.98	6.42	30.55	9.07	21.46	4.86	56.9	12.1	5.88
A Type	69	-10.55	1.02	-18.40	0.88	-7.85	0.45	39.86	8.51	24.17	7.31	15.93	3.77	49.3	11.8	4.48
W Type	60	-13.90	0.62	-24.40	0.89	-9.29	0.71	32.21	4.80	28.41	6.89	22.85	5.48	48.7	10.0	4.37
$q < 0.32$	66	-10.92	0.90	-21.58	0.96	-3.74	0.49	40.97	7.29	29.33	7.77	22.08	3.96	55.0	11.6	5.53
$q > 0.32$	63	-13.34	0.86	-20.78	0.80	-13.54	0.67	31.15	6.80	22.52	6.34	16.26	5.30	41.7	10.7	3.14
$f < 0.2$	52	-14.06	0.73	-23.16	0.31	-12.24	0.48	36.41	5.30	24.36	2.22	18.70	3.48	47.6	6.7	4.18
$f > 0.2$	57	-7.10	1.24	-23.33	1.41	-6.43	0.82	38.17	8.93	30.32	10.15	21.87	5.91	53.4	14.7	5.24
$0.2 < P \leq 0.4$	59	-14.02	0.95	-25.82	1.22	-8.57	0.79	44.00	7.33	31.64	9.37	22.15	6.06	58.6	13.6	6.18
$0.4 < P \leq 0.5$	43	-5.46	1.23	-17.29	0.55	-8.96	0.49	29.72	8.09	21.66	3.59	17.36	3.24	40.7	9.4	2.96
$P > 0.5$	27	-18.51	0.68	-17.29	0.95	-7.72	0.26	26.99	3.55	18.74	4.93	16.00	1.33	36.6	6.2	2.30
$M_{\text{tot}} < 1.60$	34	-23.26	1.44	-33.87	1.70	-10.65	0.85	48.89	8.39	39.28	9.89	26.28	4.95	68.0	13.9	7.87
$1.60 < M_{\text{tot}} \leq 1.95$	33	-5.52	0.75	-18.19	1.32	-8.61	0.95	31.62	4.31	18.86	7.61	16.36	5.48	40.3	10.3	2.90
$1.95 > M_{\text{tot}}$	35	-6.89	1.43	-16.89	0.73	-7.95	0.79	27.59	8.46	19.01	4.31	15.78	4.65	37.0	10.6	2.38
MG	27	-14.44	0.45	-14.71	0.49	-4.83	0.84	13.08	2.34	12.52	2.53	11.02	4.37	21.2	5.6	0.50
FGB	97	-11.99	0.80	-23.00	0.81	-9.22	0.49	40.92	7.86	29.31	7.97	21.45	4.80	54.7	12.2	5.47

Table 4. The parameters of the best documented moving groups.

Name	Age (M yr)	$(U, V, W)$ (km s $^{-1}$ )	$V_T$ (km s $^{-1}$ )	C.P. ( $^h$ , $^{\circ}$ )
Local Association (Pleiades, Per, M 34, Lyr, NGC 2516, IC 2602)	20 { 150	(-11.6, -21.0, 11.4)	26.5	(5.98, -35.15)
IC 2391 Supercluster (IC 2391)	35 { 55	(-20.6, -15.7, -9.1)	27.4	(5.82, -12.44)
Castor MG	200	(-10.7, -8.0, -9.7)	16.5	(4.75, -18.44)
Ursa Major Group (Sirius Supercluster)	300	(14.9, 1.0, -10.7)	18.4	(20.55, -38.10)
Hades Supercluster (Hades, Praesepe)	600	(-39.7, -17.7, -2.4)	43.5	(6.40, 6.50)

Space velocity vector of MG as a whole ( $V_T = \sqrt{U^2 + V^2 + W^2}$ ).

Direction of space velocity vector (C.P.: Converging Point in celestial coordinates).

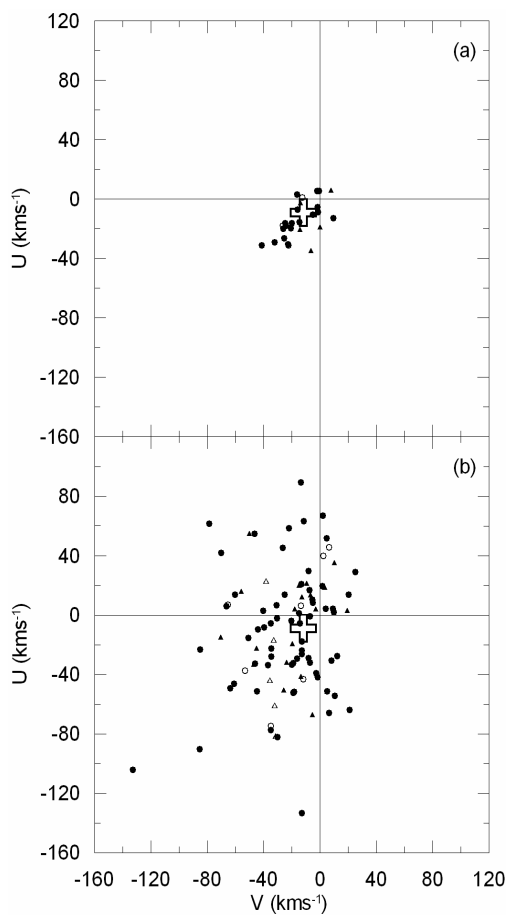


Figure 7. Distribution of (a) possible MGs and (b) FCBs on the  $(U, V)$  diagram. The position of LSR is marked by +. Symbols are the same as Fig. 1.

#### 4.3 Comparing physical parameters between FCB and MG

The kinematical criteria select out kinematically young W UMa system without a dividing line according to any physical parameter of W UMa characteristics. However, this does not mean all kinematically young W UMa's are removed from the main sample when forming the group MG. There could be systems as young as the MG group in the FCB. Those are the systems which fail to satisfy kinematical criteria although they are young. Therefore young and old all sorts of W UMa system may exist in FCB. Thus, the 5.47 Gyr kinematical age represents an average age of all stars in FCB. On the other hand, one must remember that the MG group stars are not young because of their small dispersions on the velocity space. On the contrary, their dispersions are small because they are young. They are young primarily because they are possible members of young moving groups in Table 4. Nevertheless, the word "possible" implies a limited number of non-members may well exist in MG which we believe not changes the statistic of young W UMa phenomenon.

Comparing the MG group and old CAB's, Karatas et al. (2004) found some important clues indicating mass loss and orbital period decrease in the binary evolution. A similar study is intended here to study the contact stage of the binary evolution. The physical parameters of W UMa binaries are listed in Table 5. The columns are self explanatory to indicate order number, name, apparent brightness and color ( $B-V$ ), spectral type, binary type (A or W), orbital period and inclination, masses of components, mass ratio, and over-contact parameter  $f$ . The data was primarily collected from the same literature where the radial velocities were taken. Moreover, the orbital inclinations and  $f$  values are taken from Ribulla, Reiner, & Tremko (2003) and Selam (2004).

The distribution according to spectral types are compared between the MG (younger) group and FCB (older) group in Fig. 8. It is interesting that both groups have a similar shape distribution. A slightly increased percentage of A type stars in MG group appears to be the only difference. Fig. 9 compares the orbital period distributions between MG and FCB. If one of the stars with an orbital period greater than 1 day in MG group is not counted, both groups

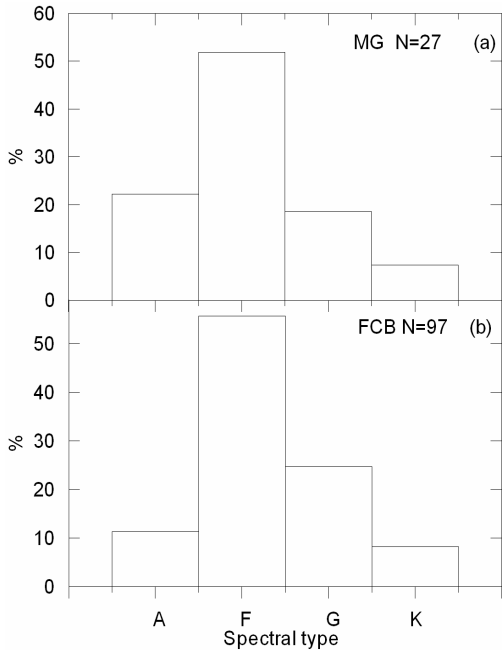


Figure 8. Comparison of spectral type histograms of (a) MGs and (b) FCBs.

cover nearly the same orbital period range ( $0.2 < P < 0.9$  days). Both groups can be said to have a peak at  $P = 0.4$  days. With 27 members the MG group has an average period  $\langle P \rangle = 0.5258$  days. With 97 members FCB group has an average period  $\langle P \rangle = 0.4275$  days. Comparing the shape of both histograms we can conclude that the relative number of longer period ( $P > 0.4$  days) systems decreased and the relative number of shorter period systems ( $P < 0.4$  days) increased in the older population sample (FCB).

These changes may appear as evidences of the period decrease in the contact binary evolution. Karatas et al. (2004) assumed the period histogram of possible MG members as the initial period distribution of old CAB. But, here, the situation is totally different. If the contact stage time scale is indeed short as estimated to be within the range  $0.1 < t_{\text{contact}} < 1$  Gyr by Guinan & Bradstreet (1988), MG contact binaries cannot be taken as an initial distribution of the FCB, because MG contact binaries will not be able to survive up to the mean kinematical age of FCB.

The mean kinematical age of FCB is 5.47 Gyr (Table 3). Karatas et al. (2004) assigned 3.86 Gyr age for the old CAB which are potential progenitors of old contact binaries (Demircan 1999). Therefore, if there is a continuous formation of CAB and evolution out of the CAB stage, some (or maybe most) of them become WUMA systems, and similarly, if the formation of WUMA systems and their evolution (coalescence) into a single star is a continuous process, and somehow if there is an equilibrium in the Galaxy, which could be investigated of course, the 1.61 Gyr age difference between old CAB and old FCB implies an upper limit for the time scale of the contact stage. Indeed, it is not much

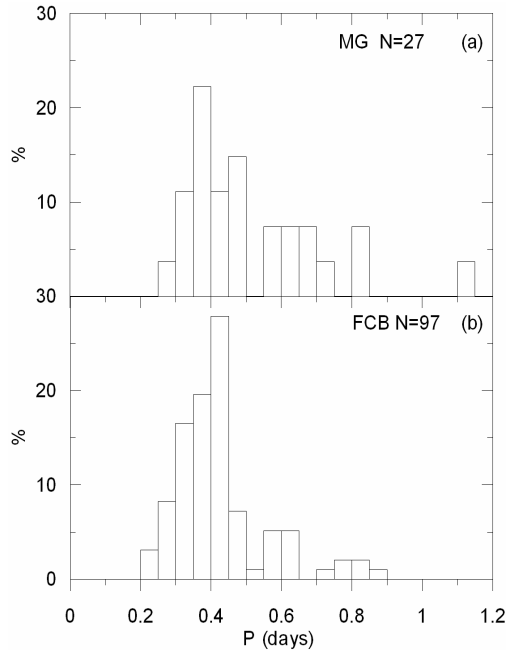


Figure 9. Comparison of period histograms of (a) MGs and (b) FCBs.

different than the estimate of  $0.1 < t_{\text{contact}} < 1$  Gyr by Guinan & Bradstreet (1988).

Therefore, it is not possible to assume the MG group to be the initial stage of the FCB group. It is most likely that the MG contact systems are formed in the beginning of the main-sequence or during the pre-main-sequence contraction phase, either by a ssion process (Roxburgh 1966) or most probably by fast spiraling in of two components in a common envelope. On the other hand, FCBs must be mostly formed from the detached progenitors.

The evidence of total mass and orbital period decrease appears to be better displayed in Table 6 where the old contact binaries are divided into four sub groups according to orbital period criterion. It is clearly displayed there that the average kinematical age increases as the orbital periods of the sub groups decrease. It is also clear that older sub groups have smaller total mass. As if, long period contact binaries in Table 6 lose mass and angular momentum, so their orbital period decrease within the time scale indicated in the Table. This scenario, however, is definitely misleading and cannot be true. This is because the age difference between the youngest and oldest sub groups in Table 6, is too long for a contact system to survive even if the empirical 1.61 Gyr time scale for the contact stage were taken into consideration.

According to the true scenario, the large dispersions (older ages) in Table 6 must have been produced not only during the contact stage, but also including the pre-contact stages before, which may be longer than the contact stage as indicated by Table 6. Thus, one should never expect, for a WUMA system in the youngest group in Table 6, to loose mass and angular momentum and join the shortest period

Table 5. Physical parameters of W UMa stars.

ID	Name	V	B - V	Spectral Type	Binary Type	P (days)	i (°)	M <sub>1</sub> (M <sub>⊙</sub> )	M <sub>2</sub> (M <sub>⊙</sub> )	q	f	Third/Multi Component
1	AQ Tuc	9.91	0.35	F 2/5	A	0.5948	80.2	1.930	0.690	0.358	0.44	
2	BH Cas	12.30	1.02	K 4V	W	0.4059	70.1	0.743	0.352	0.474	0.09	
3	DZ Psc	10.18	0.51	F 7V	A	0.3661				0.136		
4	V 523 Cas	10.62	1.05	K 4V	W	0.2337	82.0	0.637	0.319	0.501	0.20	p
5	AQ Psc	8.68	0.54	F 8V	A	0.4756				0.226		
6	AE Phe	7.56	0.64	F 8V	W	0.3624	85.3	1.366	0.629	0.461	0.17	
7	TW Cet	10.43	0.67	G 5V	W	0.3117	83.2	1.284	0.680	0.530	0.03	
8	V 776 Cas	8.94	0.52	F 2V	A	0.4404	52.5	1.723	0.225	0.130	0.70	
9	QX And	11.25	0.44	F 5V	A	0.4118	58.6	1.176	0.236	0.261	0.22	
10	SS Ari	10.37	0.62	G 0V	W	0.4060	75.3	1.343	0.406	0.302	0.13	p
11	GZ And	10.83	0.78	G 5V	W	0.3050	85.9	1.170	0.602	0.514	0.03	
12	V 376 And	7.68	0.26	A 4V	A	0.7987				0.305		
13	EE Cet	8.76	0.36	F 2V	W	0.3799	77.5	1.391	0.438	0.315	0.20	
14	UX Eri	10.50	0.67	F 9V	A	0.4453	79.0	1.366	0.510	0.373	0.00	
15	EQ Tau	10.50	0.83	G 2V	A	0.3413	86.6	1.217	0.537	0.442	0.12	p
16	BL Eri	11.50	0.63	G 0V	W	0.4169	88.0	0.609	0.330	0.542	0.16	p
17	YY Eri	8.10	0.67	G 5V	W	0.3215	82.5	1.540	0.620	0.403	0.12	
18	AO Cam	9.50	0.68	G 0V	W	0.3299	75.1	1.189	0.491	0.413	0.10	
19	RZ Tau	10.08	0.58	A 7V	A	0.4157	82.7	1.634	0.882	0.540	0.33	
20	DN Cam	8.23	0.34	F 2V	W	0.4983	71.9	1.915	0.805	0.421	0.50	
21	V 410 Aur	10.10	0.64	G 0/2V	A	0.3663	90.0	1.234	0.178	0.144	0.50	
22	V 402 Aur	8.84	0.40	F 2V	W	0.6035				0.201		
23	AP Dor	9.38	0.45	F 5V	W	0.4272	62.5			0.100	1.00	
24	V 1363 Ori	10.30	0.58	F 8V	A	0.4319				0.205	0.40	
25	ER Ori	9.28	0.49	F 7V	W	0.4234	87.5	1.385	0.765	0.552	0.15	p
26	RW Dor	10.80	0.89	K 1V	W	0.2854	76.6	0.640	0.430	0.672	0.10	
27	V 781 Tau	8.90	0.57	G 0V	W	0.3449	65.4	1.237	0.501	0.405	0.23	
28	AH Aur	10.20	0.55	F 7V	A	0.4943	75.5	1.683	0.284	0.169	0.23	
29	QW Gem	10.33	0.48	F 8V	W	0.3581	85.0	1.275	0.425	0.334	0.50	
30	V 753 Mon	8.30	0.36	A 8V	W	0.6770	74.0	1.673	1.623	0.970	0.00	
31	TY Pup	8.40	0.41	F 3V	A	0.8192	81.6	2.200	0.720	0.327	0.63	
32	FG Hya	9.90	0.64	G 2V	A	0.3278	86.8	1.414	0.157	0.112	0.74	
33	TX Cnc	10.00	0.42	F 8V	W	0.3829	62.4	0.792	0.420	0.535	0.08	
34	AH Cnc	13.31	0.53	F 5V	W	0.3604	68.0	1.290	0.540	0.419	0.41	
35	UV Lyn	9.41	0.64	F 6V	W	0.4150	66.8	1.349	0.495	0.367	0.45	
36	FN Cam	8.58	0.38	A 9V	A	0.6771	71.2	2.402	0.532	0.222	0.56	
37	EZ Hya	10.48	0.82	G 2V	W	0.4498				0.252		
38	SAnt	6.40	0.36	A 9V	A	0.6483	68.8	1.940	0.760	0.392	0.07	
39	W UMa	7.75	0.62	F 8V	W	0.3336	86.0	1.190	0.570	0.479	0.32	
40	AA UMa	10.88	0.60	F 9V	W	0.4680	80.3	1.419	0.773	0.545	0.15	
41	RT Lmi	11.40	0.60	F 7V	A	0.3749	84.0	1.298	0.476	0.367	0.23	
42	XY Leo	9.45	1.04	K 0V	W	0.2841	65.8	0.870	0.435	0.500	0.06	p
43	XZ Leo	10.60	0.38	A 8V	A	0.4877	73.3	1.892	0.659	0.348	0.02	
44	Y Sex	9.02	0.48	F 8	A	0.4198	76.8	1.210	0.220	0.182	0.00	
45	ET Leo	9.55	0.62	G 8V	W	0.3465	47.5	0.835	0.285	0.342	0.10	
46	UZ Leo	9.58	0.39	A 9V	A	0.6180	79.7	2.074	0.629	0.303	0.85	
47	EX Leo	8.27	0.53	F 6V	A	0.4086	61.1	1.557	0.309	0.199	0.31	
48	VY Sex	9.02	0.55	F 9.5	W	0.4434				0.313		
49	AM Leo	9.25	0.56	F 5V	W	0.3658	87.0	1.386	0.623	0.449	0.15	
50	VW Lmi	8.03	0.41	F 3V	A	0.4775	72.5			0.250	0.40	
51	AP Leo	9.32	0.50	F 8V	A	0.4304	77.0	1.477	0.439	0.297	0.23	
52	HNU Ma	9.90	0.59	F 8V	A	0.3826				0.140	0.20	
53	AW UMa	6.84	0.37	F 2V	A	0.4387	79.8	1.280	0.090	0.070	0.85	
54	TV Mus	11.00	0.82	F 8V	A	0.4457	78.9	1.316	0.157	0.119	0.87	
55	V 752 Cen	9.17	0.58	F 7V	W	0.3702	81.7	1.320	0.410	0.311	0.06	
56	AG Vir	8.35	0.29	A 8V	A	0.6427	80.7	1.610	0.510	0.317		
57	HX UMa	8.89	0.49	F 4V	A	0.3792	50.0	1.333	0.387	0.291	0.70	
58	CC Com	11.30	1.24	K 5V	W	0.2211	90.0	0.690	0.360	0.522	0.20	
59	AH Vir	8.89	0.81	G 8V	W	0.4075	86.5	1.360	0.412	0.303	0.24	
60	IIUMa	8.17	0.61	F 5III	A	0.8250	70.0	2.238	0.385	0.172	0.70	
61	RW Com	11.07	0.84	K 0V	W	0.2373	75.2	0.920	0.310	0.337	0.17	
62	RZ Com	10.42	0.52	F 8V	W	0.3385	86.0	1.108	0.484	0.437	0.07	
63	SX Crv	9.07	0.56	F 6V	A	0.3166				0.066		
64	BIC Vn	10.26	0.62	F 2V	A	0.3842	69.2	1.646	0.679	0.413	0.17	
65	KZ Vir	8.45	0.47	F 7V	A	1.1318				0.848		

(oldest) W UMa system s after  $t = 8.89 \times 3.21 = 5.68$  Gyr later. It is not yet clear, but it seems that when a detached system becomes a contact binary, the angular momentum loss becomes accelerated with the gravitational radiation as described by Guinan & Bradstreet (1988). If the total mass of the system does not decrease to  $t$  in the decreasing Roche lobes, then, overcontact f parameter starts to increase. The pre-contact stage, which may differ one system to system,

being much longer than the contact stage, spoils the correlation between the f parameter and the space velocity as described in Fig. 5.

Fig. 10 displays the total mass histograms of possible MG and FCB groups. Similar to the period histograms that it would be meaningless if one tries to deduce evidence of mass decrease during contact binary evolution from this figure. Therefore, it should be considered as a bare comparison

Table 5 (continued)

ID	Name	V	B - V	Spectral Type	Binary Type	P (days)	i (°)	M <sub>1</sub> (M <sub>⊙</sub> )	M <sub>2</sub> (M <sub>⊙</sub> )	q	f	Third/Multi Component
66	K R Com	7.26	0.57	G 0IV	A	0.4080				0.091	0.70	
67	H T Vir	7.06	0.56	F 8V	A	0.4077	90.0	1.258	1.022	0.812		
68	X Y Boo	10.30	0.49	F 5V	A	0.3706	69.0	0.934	0.147	0.158	0.05	
69	V 757 Cen	8.30	0.64	F 9V	W	0.3432	69.3	1.000	0.690	0.690	0.14	
70	R R Cen	7.27	0.34	A 9V	A	0.6057	78.7	1.854	0.389	0.210	0.35	
71	V W Boo	10.50	0.81	G 5V	W	0.3422	76.2	0.980	0.420	0.428	0.72	
72	N N Vir	7.64	0.41	F 0/F 1V	A	0.4807	65.0	1.794	0.882	0.491	0.50	
73	E F Boo	9.43	0.50	F 5V	W	0.4295	75.2	1.554	0.795	0.512	0.20	
74	C K Boo	8.99	0.54	F 7/8V	A	0.3552	56.6	1.788	0.198	0.111	0.14	
75	G R Vir	7.80	0.58	F 7/8V	A	0.3470				0.122		
76	A C Boo	10.00	0.59	F 8V n	W	0.3524	82.6	1.403	0.565	0.403	0.91	
77	T Y Boo	10.81	0.76	G 5V	W	0.3171	76.6	0.930	0.400	0.437	0.10	p
78	44 Boo	5.80	0.85	K 2V	W	0.2678	72.8	0.900	0.439	0.487	0.00	p
79	T Z Boo	10.41	0.63	G 2V	A	0.2972	66.9	0.783	0.104	0.133		
80	B W Dra	8.61	0.63	F 8V	W	0.2923	74.4	0.891	0.250	0.281	0.14	
81	B V Dra	7.88	0.56	F 7V	W	0.3501	76.3	0.997	0.401	0.402	0.11	
82	F I Boo	9.60	0.72	G 3V	W	0.3900				0.372	0.10	
83	O U Ser	8.25	0.64	F 9/G 0V	A	0.2968	74.3	1.018	0.176	0.173	0.31	
84	V Z Lib	10.13	0.64	G 0	A	0.3583				0.237		
85	F U Dra	10.55	0.59	F 8V	W	0.3067	78.6	1.168	0.293	0.251	0.23	
86	Y Y CrB	8.64	0.62	F 8V	A	0.3766	77.0	1.429	0.348	0.243	0.63	
87	A U Ser	10.90	0.87	K 0V	A	0.3865	80.6	0.921	0.646	0.701	0.09	
88	V 842 Her	9.85	0.65	F 9V	W	0.4190	79.0	1.360	0.353	0.260	0.25	
89	B X Dra	10.50	0.35	F 0IV -V	A	0.5790				0.289		
90	V 899 Her	7.93	0.45	F 5V	A	0.4212	68.7	1.836	1.039	0.566	0.30	
91	V 502 Oph	8.34	0.65	G 0V	W	0.4534	71.3	1.297	0.481	0.335	0.24	p
92	V 918 Her	7.30	0.28	A 7V	W	0.5748				0.271		
93	V 921 Her	9.44	0.39	A 7IV	A	0.8774	87.5	1.609	0.365	0.226	0.20	
94	V 829 Her	10.10	0.65	G 2V	W	0.3582	57.0	1.275	0.520	0.408		
95	V 2357 Oph	10.67	0.86	G 5V	A	0.4156				0.231	0.40	
96	A K Her	8.29	0.55	F 5V	A	0.4215	80.8	1.310	0.300	0.229	0.10	p
97	V 728 Her	10.90	0.41	F 3V	W	0.4713	69.2	1.654	0.295	0.178	0.71	
98	G M Dra	8.77	0.51	F 5V	W	0.3387				0.180	0.40	
99	V 2377 Oph	8.60	0.66	G 0/1V	W	0.4254				0.395	0.80	
100	V 535 Ara	7.17	0.34	A 8V	A	0.6293	82.1	1.520	0.460	0.303	0.03	
101	V 2388 Oph	6.25	0.47	F 3V	A	0.8023	83.9	1.648	0.306	0.186	0.71	
102	V 566 Oph	7.46	0.45	F 4V	A	0.4096	79.8	1.469	0.357	0.243	0.41	
103	V 972 Her	6.72	0.47	F 4V	W	0.4431				0.167	0.00	
104	V 508 Oph	10.06	0.67	F 9V	A	0.3448	86.1	1.010	0.520	0.515	0.10	
105	E F Dra	10.48	0.82	F 9V	A	0.4240	78.1	1.813	0.289	0.160	0.45	p
106	V 839 Oph	8.80	0.62	F 7V	A	0.4090	80.1	1.640	0.496	0.305	0.39	
107	eps Cra	4.74	0.40	F 2V	A	0.5914	72.3	1.720	0.220	0.128	0.30	
108	V 401 Cyg	10.64	0.38	F 0V	A	0.5827	77.0	1.679	0.487	0.290	0.46	
109	V 2082 Cyg	6.68	0.35	F 2V	A	0.7141				0.238		
110	V 417 Aql	11.00	0.53	G 2V	W	0.3703	84.5	1.395	0.505	0.362	0.19	
111	O O Aql	9.20	0.61	G 2V	A	0.5068	90.0	1.040	0.880	0.846	0.27	
112	V W Cep	7.23	0.86	G 9V	W	0.2783	63.6	0.897	0.247	0.275	0.22	
113	L S Del	8.61	0.68	G 0V	W	0.3638	48.5	1.068	0.399	0.375	0.06	
114	V 2150 Cyg	8.09	0.40	A 6V	A	0.5919				0.802	0.90	
115	H V Aqr	9.71	0.63	F 5V	A	0.3745	78.3	1.366	0.198	0.145	0.47	
116	V 1073 Cyg	8.23	0.45	F 2V	A	0.7859	68.4	1.600	0.510	0.319	0.04	
117	K P Peg	7.07	0.16	A 2V	A	0.7272				0.322		
118	D K Cyg	10.37	0.39	A 8V	A	0.4707	80.3	1.768	0.575	0.325	0.55	
119	B X Peg	11.00	0.78	G 4.5	W	0.2804	87.5	1.020	0.380	0.373	0.18	
120	V 445 Cep	6.85	0.14	A 2V	A	0.4488				0.167		
121	B B Peg	10.80	0.52	F 5V	W	0.3615	79.9	1.431	0.515	0.360	0.37	
122	V 335 Peg	7.24	0.50	F 5V	A	0.8107				0.262	0.10	
123	SW Lac	8.51	0.75	K 0V var	W	0.3207	80.2	0.959	0.779	0.851	0.39	p
124	A B And	9.50	0.87	G 8V	W	0.3319	86.8	1.005	0.494	0.560	0.15	
125	V 351 Peg	8.00	0.34	A 8V	W	0.5933	62.5	2.327	0.838	0.360	0.40	
126	V Z Psc	10.20	1.14	K 5V	A	0.2613	49.6	0.790	0.720	0.911	0.00	
127	B D + 14 5016	9.50	0.31	F 0V	A	0.6369	72.6	1.531	0.387	0.253	0.54	
128	E L Aqr	10.49	0.50	F 3V	A	0.4814	70.8	1.563	0.317	0.203		
129	U Peg	9.23	0.62	G 2V	W	0.3748	77.5	1.149	0.379	0.330	0.09	

between MG and FCB. It is the same with Fig. 11, which compares the mass ratio distribution between MG and the FCB groups. The mass ratio evolution during the contact stage cannot be deduced from Fig. 11 since MG group cannot be the initial distribution. On the other hand, all four histograms (Figs. 8, 9, 10, and 11) display an empirical evidence of contact binary evolution to indicate coalescence of WUMa systems into single stars. Otherwise, angular mo-

mentum loss does not fit in the theory of binary evolution. Then, it becomes difficult to explain why there are such differences between the MG and the FCB group WUMa stars.

A similar case also applies to the Table 6 data. We believe the age difference between MG contact binaries and the youngest FCB group in Table 6 is empirical evidence of coalescence into single stars. This is because the coalescence into a single star involves orbital period decrease as

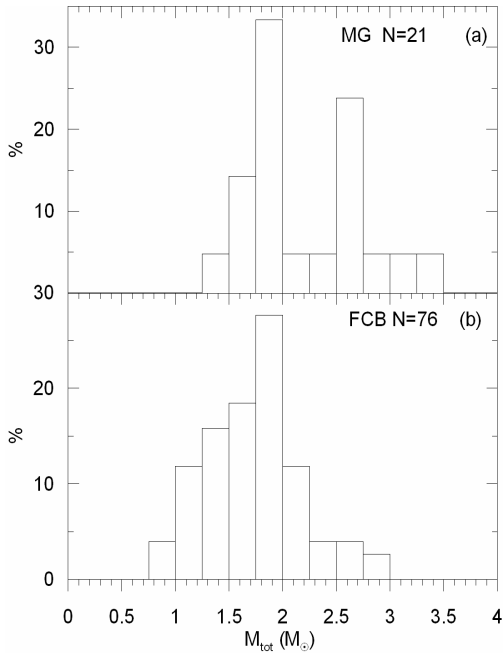


Figure 10. Comparison of the total mass ( $M_h + M_c$ ) histograms of (a) MGs and (b) FCBs.

Table 6. Kinematical ages for the period sub-groups in FCB.

P (days)	$\langle M_{\text{tot}} \rangle$ ( $M_{\odot}$ )	$\langle P \rangle$ (days)	N	$\sigma_{\text{tot}}$ ( $\text{km s}^{-1}$ )	Age (G yr)
(0.5–0.9]	2.220	0.669	17	42.09	7.1
(0.4–0.5]	1.900	0.434	34	43.86	10.4
(0.3–0.4]	1.618	0.353	35	63.90	16.0
(0.2–0.3]	1.171	0.270	11	73.92	14.6

well as angular momentum loss, most probably accelerated by gravitational radiation as described by Guinan & Bradstreet (1988) although the data in Table 6 is mostly affected by the long pre-contact stages. The derivation of the rates of orbital period decrease, mass and angular momentum loss from the present data of contact binaries requires a careful analysis and interpretation of Table 6 data. Due to limited space in this study derivation of those rates will be handled in a forthcoming study.

## 5 CONCLUSIONS

Kinematics of 129 W UMa binaries is studied. The sample is found to be heterogeneous in the velocity space that kinematically younger and older contact binaries exist in the present sample. Various sub groups are formed according to criteria involving the spectral types, binary type (A or W), mass ratio, and over-contact parameter  $f$ , orbital period and total mass. However, those criteria failed to produce kinematically homogeneous sub groups. Nevertheless, a correlation has been found to indicate shorter period and

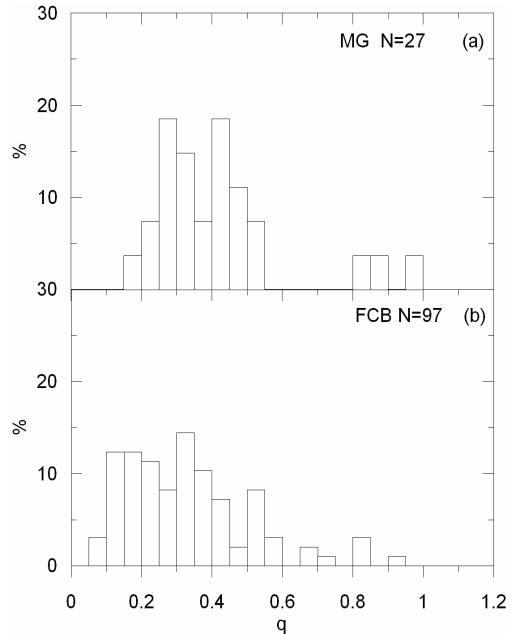


Figure 11. Comparison of the mass ratio ( $q = M_2/M_1$ , where  $M_2 < M_1$ , and  $M_1, M_2$  are the primary and secondary masses, respectively) histograms of (a) MGs and (b) FCBs.

less massive systems show larger velocity dispersions than longer period more massive systems. The mean kinematical ages of all sub groups are estimated from the velocity dispersions using the tables of Weilen (1982) and listed in Table 3.

The possible moving group members among the present W UMa stars are investigated according to the kinematical criteria originally defined by Eggen (1958a, b, 1989, 1995) and 28 W UMa are found to be a possible member of five best documented MGs which are summarized in Table 4. The group of the old contact binaries (FCB) is formed by removing out the possible moving group members and the W UMa systems which are known to be the members of known open clusters from the main sample. The 5.47 G yr mean kinematical age is estimated for the old contact systems (FCB). The age difference is found to be 1.61 G yr between the 3.86 G yr old CAB (Karatas et al. 2004) and the FCB. If there is a number equilibrium between the CAB and FCB established by the evolution, the upper limit of the lifetime of the contact stage can be estimated as 1.61 G yr which is in close agreement with the estimation made by Guinan & Bradstreet (1988) as  $0.1 < t_{\text{contact}} < 1$  G yr.

Since the contact stage appears to be very short in comparison with the mean kinematical age of FCB, the group containing possible MG stars cannot be used as an initial subsample of FCB. Thus, the histograms (Figs. 8, 9, and 10) and ages of sub groups of FCB according to orbital ranges (Table 6) cannot be used directly to deduce evidence of period decrease and angular momentum loss during contact stage evolution. Nevertheless, since, those histograms and data in Table 6, cannot be explained without angular momentum

loss and orbital period decrease in binary evolution, and since it is illogical to assume that angular momentum loss and orbital period decrease operate only for the pre-contact stages, the angular momentum loss and the orbital period decrease are evidently occurring as predicted by Guinan & Bradstreet (1988) even if one cannot deduce them directly from those histograms and Table 6.

We have found 27 systems to form the MG group. Existences of MG members is an exciting (perhaps the most exciting) finding of this study. This is because these WUM systems do not have enough ages to be formed from detached binary progenitors by the mechanism involving angular momentum loss and orbital period decrease. In fact the age difference between the youngest FCB sub group (3.21 Gyr, in Table 6) and MG group (0.5 Gyr, in Table 3) is more than lifetime (1.61 Gyr) of the contact stage. Therefore, it could be concluded that the MG contact systems are formed in the beginning of the main-sequence or during the pre-main-sequence contraction phase, either by a session process (Roxburgh 1966) or by fast spiraling the two components in a common envelope. As a result, it can be said that detached binary progenitors, presumably short period ( $P < 5$  days) RS CVn binaries, are not the only source from which WUM systems could be formed by the mechanism involving angular momentum loss and orbital period decrease. It is indeed a challenge to disprove true membership of MG stars in our list. This may not be enough, one also needs to prove their ages to be bigger than our estimate, that is, their ages must be proven to be big enough (bigger than the pre-main sequence contraction plus the contact stage lifetime) then one can claim the detached binary progenitors are the only source to form WUM systems.

## 6 ACKNOWLEDGMENTS

This research has made use of the SIMBAD database, operated at CDS, Strasbourg, France. Thanks to B. J. Hrivnak for providing private communications. We also thank to D. R. Slavek Rucinski for his substantial input into the paper as the referee. A British national, who is an English teacher, Margaret Kadoglu helped on the grammar and linguistics. This work was supported by the Research Fund of the University of Istanbul. Project number 244/23082004.

## REFERENCES

- Ahn Y. S., Hill G., Khalessah B., 1992, *A & A*, 265, 597  
 Aksan Z., Ðzdemir T., Yesilyaprak C., Ðskender A., 1999, *Tr. J. of Physics*, 23, 45  
 Bartkevičius A., Lazauskaite R., Bartasiute S., 1999, Harmonizing Cosmic Distance Scales in a Post-Hipparcos Era, ASTR Conference Series, Vol. 167. Edited by Daniel Egret, & Andre Heck, p. 247-250  
 Batten A. H., Lu W., 1986, *PA SP*, 98, 92  
 Bell S. A., Rainger P. P., Hilditch R. W., 1990, *MNRAS*, 247, 632  
 Binneindijk L., 1970, *Vistas in Astronomy*, 12, 217  
 Bopp B. W., Rucinski S. M., 1981, in *Fundamental Problems in the Theory of Stellar Evolution*, IAU Symp. No. 93, eds. D. Sugimoto et al. (Dordrecht-Reidel), p. 177  
 Bopp B. W., Stencel R. E., 1981, *ApJ*, 247L, 131  
 Buser R., Rong J., Karaali S., 1999, *A & A*, 348, 98  
 Cernutti M. A., Nienella V. S., 1982, *PA SP*, 94, 195  
 Demircan O., 1999, *Tr. J. of Physics*, 23, 425  
 Demircan O., Eker Z., Karatas Y., Bilir S., 2004, in preparation  
 Duerbeck H. W., 1978, *Aca*, 28, 49  
 Eggen O. J., 1958a, *MNRAS*, 118, 65  
 Eggen O. J., 1958b, *MNRAS*, 118, 154  
 Eggen O. J., 1989, *PA SP*, 101, 366  
 Eggen O. J., 1994, in Morrison L. V., Gilmore G., eds, *Galactic and Solar System Optical Asterometry*. Cambridge Univ. Press, Cambridge, p. 191  
 Eggen O. J., 1995, *AJ*, 110, 2862  
 Eker Z., 1992, *ApJS*, 79, 481  
 ESA, 1997, *The Hipparcos and Tycho Catalogues*, ESA SP-1200  
 Gatewood G., de Jonge J. K., 1994, *ApJ*, 428, 166  
 Gatewood G., 1995, *ApJ*, 445, 712  
 Green E. M., Demarque P., King C. R., 1987, *The revised Yale Isochrones*, Yale Univ. Obs., New Haven.  
 Goedeking K. D., Duerbeck H. W., 1993, *A & A*, 278, 463  
 Goedeking K. D., Duerbeck H. W., Plewa T., Kaluzny J., Schertl D., Weigelt G., Flin P., 1994, *A & A*, 289, 827  
 Gronon M., 1987, *JAA*, 8, 123  
 Guinan E. F., Bradstreet D. H., 1988, in: *Formation and Evolution of Low Mass Stars*, A. K. Dupree and M. T. Lago, eds., Kluwer, Dordrecht, p. 345  
 Hilditch R. W., King, D. J., 1986, *MNRAS*, 223, 581  
 Hilditch R. W., King, D. J., McFarlane T. M., 1989, *MNRAS*, 237, 447  
 Hilditch R. W., Hill G., Bell S. A., 1992, *MNRAS*, 255, 285  
 Hog E., Kuzmin A., Bastian U., Fabricius C., Kuijken K., Lindgren L., Makarov V. V., Roosnor S., 1998, *A & A*, 335L, 65  
 Hog E., Fabricius C., Makarov V. V., Urban S., Corbin T., Wycoff G., Bastian U., Schweikart P., Wienec A., 2000, *A & A*, 355L, 27  
 Hill G., Barnes J. V., 1972, *PA SP*, 84, 382  
 Hill G., 1989, *A & A*, 218, 141  
 Hill G., Fisher W. A., Holmgren D., 1989, *A & A*, 218, 152  
 Hrivnak B. J., Milone E. F., Hill G., Fisher W. A., 1984, *ApJ*, 285, 683  
 Hrivnak J., 1989, *ApJ*, 340, 458  
 Hrivnak B. J., Milone E. F., 1989, *AJ*, 97, 523  
 Hrivnak B. J., 1993, *New frontiers in binary star research: a colloquium sponsored by the U.S. National Science Foundation and the Korean Science and Engineering Foundation*, Seoul and Taejon, Korea, November 5-13, 1990. Edited by Kam-Ching Leung and Il-Seong Nha. San Francisco, Calif. Astronomical Society of the Pacific, p. 269  
 Huang S. S., 1967, *ApJ*, 150, 229  
 Jeries R. D., 1995, *MNRAS*, 273, 559  
 Johnson D. R. H., Soderblom D. R., 1987, *AJ*, 93, 864  
 Joy A. H., 1926, *ApJ*, 64, 287  
 Karatas Y., Bilir S., Eker Z., Demircan O., 2004, *MNRAS*, 349, 1069  
 Karaali S., Bilir S., Hamzaoglu E., 2004, *MNRAS*, 355, 307  
 King D. J., Hilditch R. W., 1984, *MNRAS*, 209, 645  
 King J. R., Villareal A. R., Soderblom D. R., Gulliver A. F., Adelman, S. J., 2003, *AJ*, 125, 1980  
 Kukarkin B. V., Kholopov P. N., Pskovsky Y. K., Efremov Y. N., Kukarkina N. P., Kurochkin N. E., Medvedeva G. I., 1971, *GCVS*, 3rd ed. (1971)  
 Lu W., 1985, *PA SP*, 97, 1086  
 Lu W., 1986, *PA SP*, 98, 577  
 Lu W., 1988a, *AcApS*, 8, 26  
 Lu W., 1988b, *AcApS*, 8, 259  
 Lu W., 1991, *AJ*, 102, 262  
 Lu W., 1993, *AJ*, 105, 646  
 Lu W., Rucinski S. M., 1993, *AJ*, 106, 361  
 Lu W., Rucinski S. M., 1999, *AJ*, 118, 515  
 Lu W., Rucinski S. M., Ogleza W., 2001, *AJ*, 122, 402  
 Maceroni C., 1986, *A & A*, 170, 43

- Maceroni C., van't Veer F., 1996, *A & A*, 311, 523  
 Maciejewski G., Ligeza P., Karska A., 2003, *IBVS*, 5400, 1  
 Marsakov V. A., Shevchenko Y. G., 1995, *Bull. Inf. Centre D'onnees Stellaires*, Vol. 47, p.13  
 McLean B. J., 1981, *MNRAS*, 195, 931  
 McLean B. J., Hilditch R. W., 1983, *MNRAS*, 203, 1  
 McLean B. J., 1983, *MNRAS*, 204, 817  
 Mestel L., 1968, *MNRAS*, 138, 359  
 Metcalfe T. S., 1999, *AJ*, 117, 2503  
 Michaelis D., Binney J., 1981, *Galactic Astronomy: Structure and Kinematics*, 2nd edition  
 Milone E. F., Hrivnak B. J., Hill G., Fisher W. A., 1985a, *AJ*, 90, 109  
 Milone E. F., Hrivnak B. J., Fisher W. A., 1985b, *AJ*, 90, 354  
 Milone E. F., Stagg C. R., Sugars B. A., McLean J. R., Schiller S. J., Kallrath J., Bradstreet D. H., 1995, *AJ*, 109, 359  
 Montes D., Lopez-Santiago J., Gavez M. C., Fernandez-Figueroa M. J., De Castro E., Comide M., 2001a, *MNRAS*, 328, 45  
 Montes D., Fernandez-Figueroa M. J., De Castro E., Comide M., Latorre A., 2001b, 11th Cambridge Workshop on Cool Stars, Stellar Systems and the Sun, ASP Conference Proceedings, Vol. 223. Edited by Ramon J. Garcia Lopez, Rafael Rebolo, & Maria Rosa Zapatero Osorio. San Francisco: Astronomical Society of the Pacific, p.1477  
 Moore J. H., Paddock G. F., 1950, *ApJ*, 112, 48  
 Montgomery K. A., Marschall L. A., Janes K. A., 1993, *AJ*, 106, 181  
 Nelson R. H., Milone E. F., Vanleeuwen J., Terrell D., Penfold J. E., Kallrath J., 1995, *AJ*, 110, 2400  
 Nesic R., Maceroni C., Milano L., Russo G., 1986, *A & A*, 159, 142  
 Nordstrom B., Mayor M., Andersen J., Holmberg J., Pont F., Jorgensen B. R., Olsen E. H., Udry S., Mowlavi N., 2004, *A & A*, 418, 989  
 Okamoto I., Sato K., 1970, *PA SJ*, 22, 317  
 Pashouresh R., Edalati, M. T., 2003, *Ap&SS*, 288, 259  
 Perrymann M. A. C., Lindgren L., Kovalevsky J., Hog E., Bastian U., Bernacca P. L., Creze M., Donati F., Grenon M., van Leeuwen F., nine coauthors, 1997, *A & A*, 323L, 49  
 Pavlov M., 1968, *A dv. Astron. Astrophys.*, 6, 201  
 Ribulla T., Kreiner J. M., Trenko J., 2003, *Coska*, 33, 38  
 Przybylska M., Orris, K. P., 1965, *MNRAS*, 129, 63  
 Pych W., Rucinski S. M., Debond H., Thompson J. R., Capobianco C. C., Blake R. M., Oglezna W., Stachowski G., Rogozinski P., Ligeza P., Gazeas K., 2004, *AJ*, 127, 1712  
 Rainger P. P., Hilditch R. W., Bell S. A., 1990a, *MNRAS*, 246, 42  
 Rainger P. P., Bell S. A., Hilditch R. W., 1990b, *MNRAS*, 246, 47  
 Roese S., Bastian U., 1988, *A & AS*, 74, 449  
 Roxburgh I. W., 1966, *ApJ*, 143, 111  
 Rucinski S. M., Whelan J. A. J., Worden S. P., 1977, *PA SP*, 89, 684  
 Rucinski S. M., Lu W. X., Shi J., 1993, *AJ*, 106, 1174  
 Rucinski S. M., Lu W., 1999, *AJ*, 118, 2451  
 Rucinski S. M., Lu W., Mochnicki S. W., 2000, *AJ*, 120, 1133  
 Rucinski S. M., Lu W., Mochnicki S. W., Oglezna W., Stachowski G., 2001, *AJ*, 122, 1974  
 Rucinski S. M., Lu W., Capobianco C. C., Mochnicki S. W., Blake R. M., Thompson J. R., Oglezna W., Stachowski G., 2002, *AJ*, 124, 1738  
 Rucinski S. M., Capobianco C. C., Lu W., Debond H., Thompson J. R., Mochnicki S. W., Blake R. M., Oglezna W., Stachowski G., Rogozinski P., 2003, *AJ*, 125, 3258  
 Rucinski S. M., 2004, *NewAR*, 48, 703  
 Samec R. G., Hube D. P., 1991, *AJ*, 102, 1171  
 Sanford R. F., 1934, *ApJ*, 79, 89  
 Schonele E., 1979, *A & AS*, 36, 287  
 Selam S. O., 2004, *A & A*, 416, 1097  
 Siegel M. H., Maciejewski S. R., Reid I. N., Thompson I. B., 2002, *ApJ*, 578, 151  
 Sistero R. F., Castore de Sistero M. E., 1974, *AJ*, 79, 391  
 Struve O., 1950, *ApJ*, 112, 184  
 Struve O., Horak H. G., Canavaggio R., Kourganoff V., Colacevich A., 1950, *ApJ*, 111, 658  
 Thomas H. S., 1977, *ARA & A*, 15, 127  
 van't Veer F., 1975, *A & A*, 40, 167  
 van't Veer F., 1979, *A & A*, 80, 287  
 Vilhu O., Rahunen T., 1980, *IAU Symposium* 88, eds. M. J. Plavec et al. (Dordrecht: Reidel), p.491  
 Whelan J. A. J., Romanishin W., Worden S. P., Rucinski S. M., 1979, *MNRAS*, 186, 729  
 Wielen R., 1982, *Landolt-Bornstein Tables, Astrophysics*, 2C, Sec. 8.4, 29, Table 8  
 Yamazaki A., Jugaku J., Seki M., 1988, *AJ*, 95, 894  
 Zhai D., Lu W., 1989, *AcApS*, 9, 208